

Relic densities of dark matter in the U(1)-extended NMSSM and the gauged axion supermultiplet

Claudio Corianò,^{1,*} Marco Guzzi,^{2,†} and Antonio Mariano^{1,‡}

¹*Dipartimento di Matematica e Fisica, Università del Salento and INFN Sezione di Lecce, Via Arnesano 73100 Lecce, Italy*

²*Department of Physics, Southern Methodist University, Dallas, Texas 75275, USA*

(Received 26 April 2011; revised manuscript received 20 January 2012; published 15 May 2012)

We compute the dark matter relic densities of neutralinos and axions in a supersymmetric model with a gauged anomalous U(1) symmetry. The model is a variant of the USSM [the U(1) extended NMSSM], containing an extra U(1) symmetry and an extra singlet in the superpotential with respect to the MSSM, where gauge invariance is restored by Peccei-Quinn interactions using a Stückelberg multiplet. This approach introduces an axion (Im*b*) and a saxion (Re*b*) in the spectrum and generates an axino component for the neutralino. The Stückelberg axion (Im*b*) develops a physical component (the gauged axion) after electroweak symmetry breaking. We classify all the interactions of the Lagrangian and perform a complete simulation study of the spectrum, determining the neutralino relic densities using MICROMEAS. We discuss the phenomenological implications of the model analyzing mass values for the axion from the milli-eV to the MeV region. These depend sensitively on the value of $\tan\beta$. The possible scenarios that we analyze are significantly constrained by a combination of WMAP data, the exclusion limits from direct axion searches, and the veto on late entropy release at the time of nucleosynthesis.

DOI: [10.1103/PhysRevD.85.095008](https://doi.org/10.1103/PhysRevD.85.095008)

PACS numbers: 95.35.+d, 12.60.Jv

I. INTRODUCTION

Axions have been studied along the years both as a realistic attempt to solve the strong *CP* problem [1–8], to which they are closely related, but also as a possible candidate to answer more recent puzzles in cosmology, such as the origin of dark energy, whose presence has found confirmation in the study of type I supernovae [9,10]. In this second case it has been pointed out that they can contribute to the vacuum energy, a possibility that remains realistic if their mass m_a —which in this case should be $\sim 10^{-33}$ eV and smaller—is of electroweak (EW) [11] and not of QCD origin. In this case they differ significantly from the standard (Peccei-Quinn, PQ) invisible axion.

According to this scenario, the vacuum misalignment (see [12,13] for a discussion in the PQ case) induced at the electroweak scale would guarantee that the degree of freedom associated with the axion field remains frozen, rolling down very slowly toward the minimum of the non-perturbative instanton potential, with m_a much smaller than the current Hubble rate. Given the rather tight experimental constraints which have significantly affected the parameter space (axion mass and gauge couplings) for PQ axions [14–16], the study of these types of fields has also taken into account the possibility to evade the current bounds [17,18]. These are summarized into both an upper and a lower bound on the size of f_a , the axion decay constant, which sets the scale of the misalignment angle θ , defined as the ratio of the axion field (a) over the PQ scale v_{PQ} ($v_{\text{PQ}} \sim f_a$).

Axionlike particles can be reasonably described by pseudoscalar fields characterized by an enlarged parameter space for mass and couplings, with a direct coupling to the gauge fields (of the form $aF\tilde{F}$) whose strength remains unrelated to their mass. They have been at the center of several recent and less recent studies (see for instance [18–25]). They are supposed to inherit most of the properties of a typical invisible axion—a PQ axion—while acquiring some others which are not allowed to it.

We recall that the axion mass [which in the PQ case is $O(\Lambda_{\text{QCD}}^2/f_a)$] and the axion coupling to the gauge fields are indeed related by the same constant f_a . In the PQ case f_a ($\sim 10^{10}$ – 10^{12} GeV) makes the axion rather light ($\sim 10^{-3}$ – 10^{-5} eV) and also very weakly coupled. The same (large) scale plays a significant role in establishing the axion as a possible dark matter candidate, contributing significantly to the relic densities of cold dark matter. A much smaller value of f_a , for instance, would diminish significantly the axion contribution to cold dark matter due to the suppression of its abundance (Y_χ) which depends quadratically on f_a .

It is quite immediate to realize that the gauging of the axionic symmetries by introducing a local anomalous U(1)—inherited from an underlying anomalous structure, i.e. a gauge anomaly—allows one to leave the mass and the coupling of the axion to the gauge fields unrelated [26,27], offering a natural theoretical justification for the origin of axionlike particles. We recall that effective low energy models incorporating gauged PQ interactions emerge in several string and supergravity constructions, for instance in orientifold vacua of string theory and in gauged supergravities (see for instance [28,29]).

*claudio.coriano@unisalento.it

†mguzzi@physics.smu.edu

‡antonio.mariano@unisalento.it

The analysis that we perform in this work has the goal to capture the relevant phenomenological features of the axions present in this class of models, extending a previous study presented in a nonsupersymmetric context [30]. We will be following, as in previous studies, a bottom-up approach. This allows one to identify the low energy effective action on the basis of a rather simple operatorial structure typical of anomalous Abelian models. The theory is then fixed by the condition of gauge invariance of the anomalous effective action, amended by operators of dimension-5 [Wess-Zumino (WZ) or PQ-like terms] which appear in the action suppressed by a suitable scale, the Stückelberg mass (M_{St}).

The introduction of the Stückelberg multiplet (or axion multiplet), while necessary for the restoration of gauge invariance, is in general expected to raise some concerns at the cosmological level because of the presence, among its components, of a scalar modulus, the saxion. In supersymmetric (ordinary) PQ formulations this has a mass of the order of the weak scale or smaller and poses severe problems to the standard cosmological scenario. A late time decay of this particle, for instance, could cause an entropy release with a low reheating temperature ($T_{\text{RH}} < 5 \text{ MeV}$) which is unacceptable for nucleosynthesis. For comparison, we mention that in the case of string moduli, for instance, the interaction of these states with the rest of the fields of the low energy spectrum is suppressed by the Planck scale. In turn, this forces the mass of these states to be quite large (100 TeV or so) [31,32] in order to enhance the phase space for their decay, for a similar reason.

In our construction the scalar modulus of the axion multiplet acquires a mass of the order of the Stückelberg scale and has sizable interactions with the other fields of the model, thereby decaying pretty fast ($\sim 10^{-23} \text{ s}$). Therefore, smaller values of its mass—in the TeV range—turn out to be compatible with the standard scenario for nucleosynthesis.

Nonsupersymmetric versions of the class of models that we are going to analyze have been discussed in detail in [26,27,33]. Recently [34,35], an extension of a specific supersymmetric model, the USSM [the U(1)-extended next-to-minimal supersymmetric standard model of [36]] has been presented, in which the U(1) symmetry is anomalous. This model supports an axionlike particle in its spectrum. It has been named the “USSM-A,” to recall both its supersymmetric origin and its anomalous Abelian gauge structure. It is also close to a similar U(1)' extension of the MSSM [the U(1)' minimal supersymmetric standard model] [37], which supports an axino component among the interaction eigenstates of the neutralino sector, but not a gauged axion, due to the structure of the MSSM superpotential. The study of relic densities in this model have been performed in [38,39]. In the nonsupersymmetric case the identification of a physical axion in the spectra of these models has been discussed in detail in [33],

a realization called “the minimal low scale orientifold model” or MLSOM for short.

Both in the USSM-A and in the model of [37], the extra U(1) symmetry takes an anomalous form and the violation of gauge invariance requires supersymmetric PQ interactions, with a Stückelberg supermultiplet for the restoration of the gauge symmetry. The extra gauge boson of the anomalous U(1) symmetry is massive and in the Stückelberg phase, as in previous nonsupersymmetric constructions [26,27,33]. As shown in the case of the MLSOM, axionlike particles appear in the CP -odd spectrum of these theories whenever Higgs-axion mixing [33] occurs. For this reason in this work we will be using the term “gauged supersymmetric axion” (or axi-Higgs, denoted equivalently as χ or H_0^5) to refer to this state.

As we have mentioned in the Introduction, we will follow a minimal approach. This approach allows one to define an effective theory on the basis of (1) an assigned gauge structure (the number of anomalous Abelian interactions); (2) some conditions of anomaly cancellation and gauge invariance of the effective Lagrangian; and (3) the choice of a suitable value of the Stückelberg mass scale characterizing the range in which the description of these effective models is compatible with unitarity [40]. As in a previous analysis for the LHC in the MLSOM [41], we will first stress the general features of these models, deriving the defining conditions for the counterterms which appear in the structure of the effective action, before moving to a specific realization with a selected charge assignment. In our simulations we have found that the dependence of the results on the choices of the independent charges is, however, extremely mild. In this respect the properties that we are able to extrapolate from this class of models—even with a single charge assignment—are pretty general and depend quite sensitively only on the choice of the Stückelberg mass M_{St} and the MSSM Higgs vacuum expectation value (VEV) ratio $\tan\beta$.

In this section we will focus on the axion/saxion Lagrangian, leaving a general discussion of the various contributions to Appendix A. It is given by

$$\mathcal{L}_{\text{axion/saxion}} = \mathcal{L}_{\text{St}} + \mathcal{L}_{\text{WZ}}, \quad (1)$$

where \mathcal{L}_{St} is the supersymmetric version of the Stückelberg mass term [42], while \mathcal{L}_{WZ} denotes the WZ counterterms responsible for the axionlike nature of the pseudoscalar b . Specifically

$$\begin{aligned} \mathcal{L}_{\text{St}} &= \frac{1}{2} \int d^4\theta (\hat{\mathbf{b}} + \hat{\mathbf{b}}^\dagger + \sqrt{2}M_{\text{St}}\hat{B})^2, \\ \mathcal{L}_{\text{WZ}} &= -\frac{1}{2} \int d^4\theta \left\{ \left[\frac{c_G}{M_{\text{St}}} \text{Tr}(\mathcal{G}\mathcal{G})\hat{\mathbf{b}} + \frac{c_W}{M_{\text{St}}} \text{Tr}(WW)\hat{\mathbf{b}} \right. \right. \\ &\quad + \frac{c_Y}{M_{\text{St}}} \hat{\mathbf{b}} W_\alpha^Y W^{Y,\alpha} + \frac{c_B}{M_{\text{St}}} \hat{\mathbf{b}} W_\alpha^B W^{B,\alpha} \\ &\quad \left. \left. + \frac{c_{YB}}{M_{\text{St}}} \hat{\mathbf{b}} W_\alpha^Y W^{B,\alpha} \right] \delta(\bar{\theta}^2) + \text{H.c.} \right\}, \quad (2) \end{aligned}$$

where we have denoted with \mathcal{G} the supersymmetric field strength of $SU(3)_c$, with W the supersymmetric field strength of $SU(2)$, with W^Y and with W^B the supersymmetric field strength of $U(1)_Y$ and $U(1)_B$, respectively. The Lagrangian \mathcal{L}_{St} is invariant under the $U(1)_B$ gauge transformations

$$\delta_B \hat{B} = \hat{\Lambda} + \hat{\Lambda}^\dagger, \quad \delta_B \hat{\mathbf{b}} = -2M_{St} \hat{\Lambda}, \quad (3)$$

where $\hat{\Lambda}$ is an arbitrary chiral superfield. So the scalar component of $\hat{\mathbf{b}}$, that consists of the saxion and the axion field, shifts under a $U(1)_B$ gauge transformation. The coefficients $c_I \equiv (c_G, c_W, c_Y, c_B, c_{YB})$ are dimensionless, fixed by the conditions of gauge invariance, and are functions of the free charges B_i of the model [as shown in Eq. (5)]. Extracting the group factors we have

$$\begin{aligned} c_B &= -\frac{\mathcal{A}_{BBB}}{384\pi^2}, & c_Y &= -\frac{\mathcal{A}_{BYY}}{128\pi^2}, \\ c_{YB} &= -\frac{\mathcal{A}_{BBY}}{128\pi^2}, & c_W &= -\frac{\mathcal{A}_{BWW}}{64\pi^2}, \\ c_G &= -\frac{\mathcal{A}_{BGG}}{64\pi^2}. \end{aligned} \quad (4)$$

The coefficients \mathcal{A} are defined by the conditions of gauge invariance of the effective action, related to the anomalies $\{U(1)_B^3\}$, $\{U(1)_B, U(1)_Y^2\}$, $\{U(1)_B^2, U(1)_Y\}$, $\{U(1)_B, SU(2)^2\}$, and $\{U(1)_B, SU(3)^2\}$. Using the conditions of gauge invariance these coefficients assume the form

$$\begin{aligned} \mathcal{A}_{BBB} &= -3B_{H_1}^3 - 3B_{H_1}^2(3B_L + 18B_Q - 7B_S) \\ &\quad - 3B_{H_1}(3B_L^2 + (18B_Q - 7B_S)B_S) \\ &\quad + 3B_L^3 + B_S(27B_Q^2 - 27B_S B_Q + 8B_S^2), \\ \mathcal{A}_{BYY} &= \frac{1}{2}(-3B_L - 9B_Q + 7B_S), \\ \mathcal{A}_{BBY} &= 2B_{H_1}(3B_L + 9B_Q - 5B_S) + (12B_Q - 5B_S)B_S, \\ \mathcal{A}_{BWW} &= \frac{1}{2}(3B_L + 9B_Q - B_S), \quad \mathcal{A}_{BGG} = \frac{3}{2}B_S. \end{aligned} \quad (5)$$

We have expressed all the anomaly equations in terms of 4 charges $B_i \equiv (B_{H_1}, B_S, B_Q, B_L)$ ordered from 1 to 4 (left to right). Notice that these charges can be taken as fundamental parameters of the model. Their independent variation allows one to scan the entire spectra of these models with no reference to any specific construction. These relations appear in the anomalous variation (δ_B) of the supersymmetric 1-loop effective action of the model, which forces the introduction of supersymmetric PQ-like interactions (WZ terms) for its overall vanishing. Formally we have the relation

$$\delta_B(B_i)\mathcal{S}_{1\text{loop}} + \delta_B(c_I(B_i))\mathcal{S}_{WZ} = 0, \quad (6)$$

where the anomalous variation can be parametrized by the 4 charges B_i together with the coefficients $c_J(B_i)$ in front of the WZ counterterms. In these notations, the uppercase index J runs over all the 5 mixed-anomaly conditions

B^3 , BY^2 , B^2Y , BW^2 , and BG^2 , ordered from 1 to 5 (left to right). Before coming to the definition of the charge assignments we pause for a remark. As we are going to show in the next sections, the scalar potential takes a non-local form unless all the anomaly coefficients in Eq. (5) are zero. Such potential can however be expanded in powers of Reb/M_{St} , and as such these contributions turn out to be irrelevant if M_{St} is a very large scale. The situation is rather different if M_{St} is bound to lay around the 1 TeV region, where the potential could actually develop a singularity. In fact, in this case, it is in general expected that a singular potential will soon dominate the dynamics of the model.

We will give the explicit expression of the D terms for a general choice of the counterterms. The function (f) which allows one to identify all the charges in terms of the free ones is formally given by

$$f(B_Q, B_L, B_{H_1}, B_S) = (B_Q, B_{U_R}, B_{D_R}, B_L, B_R, B_{H_1}, B_{H_2}, B_S). \quad (7)$$

These depend only upon the 4 free parameters B_Q, B_L, B_{H_1} , and B_S . In our analysis, the charges of Eq. (7) have been assigned as

$$f(2, 1, -1, 3) = (2, 0, -1, 1, 0, -1, -2, 3). \quad (8)$$

As we have already mentioned, the dependence of our results on this choice of parametric charges is very small. Instead, as we will see, the relevant parameters of our analysis turn out to be (1) the anomalous coupling of the gauge boson g_B , which controls the decay rate of the saxion and of the axion, and (2) the Stückelberg mass.

II. AXIONS, SAXIONS, AND ALL ORDERS INTERACTIONS

The contributions of the axion and saxion to the total Lagrangian are derived from the combination of the Stückelberg and Wess-Zumino terms. The complete axion/saxion Lagrangian expressed in terms of component fields is given by

$$\mathcal{L}_{\text{axion/saxion}} \equiv \mathcal{L}_{St} + \mathcal{L}_{WZ} \quad (9)$$

and contains a mixing among the D terms which is rather peculiar, as we are going to show. The off-shell expression of this Lagrangian is given by

$$\begin{aligned} \mathcal{L}_{\text{axion/saxion}} &= \frac{1}{2}(\partial_\mu \text{Im}b + M_{St}B_\mu)^2 + \frac{1}{2}\partial_\mu \text{Re}b\partial^\mu \text{Re}b \\ &\quad + \frac{i}{2}\psi_{\mathbf{b}}\sigma^\mu\partial_\mu\bar{\psi}_{\mathbf{b}} + \frac{i}{2}\bar{\psi}_{\mathbf{b}}\bar{\sigma}^\mu\partial_\mu\psi_{\mathbf{b}} \\ &\quad + F_{\mathbf{b}}^\dagger F_{\mathbf{b}} + \mathcal{L}_{\text{axion},i}, \end{aligned} \quad (10)$$

where the expression of $\mathcal{L}_{\text{axion},i}$ is quite lengthy and can be found in Appendix A [Eq. (A10)].

The equation of motion for the auxiliary field $F_{\mathbf{b}}$ can be derived quite immediately and give for the F term of the Stückelberg field the expression

$$F_{\mathbf{b}} = -\frac{1}{16} \frac{c_G}{M_{\text{St}}} \bar{\lambda}_G^a \bar{\lambda}_G^a - \frac{1}{16} \frac{c_W}{M_{\text{St}}} \bar{\lambda}_W^i \bar{\lambda}_W^i - \frac{1}{2} \frac{c_Y}{M_{\text{St}}} \bar{\lambda}_Y \bar{\lambda}_Y - \frac{1}{2} \frac{c_B}{M_{\text{St}}} \bar{\lambda}_B \bar{\lambda}_B + \frac{1}{2} \frac{c_{YB}}{M_{\text{St}}} \bar{\lambda}_Y \bar{\lambda}_B. \quad (11)$$

One important feature of the supersymmetric model is that b is a complex field with its real and imaginary parts. While $\text{Im}b$ may appear in the CP -odd part of the scalar sector and undergoes mixing with the Higgs sector, its real part, $\text{Re}b$, the saxion (or scalar axion) before the EW symmetry breaking, has a mass exactly equal to the Stückelberg mass, as expected from supersymmetry. We recall that in the absence of supersymmetry (SUSY) breaking parameters, the components of the Stückelberg multiplet form, together with the vector multiplet of the anomalous gauge boson, a massive vector multiplet of mass M_{St} . This is composed of the massive anomalous gauge boson, whose mass is given by the Stückelberg term, the massive saxion, and a massive Dirac fermion of mass M_{St} . The fermion is obtained by diagonalizing the 2-dimensional mass matrix constructed in the basis of λ_B —the gaugino from the vector multiplet \hat{B} —and ψ_b , which is the axino of the Stückelberg multiplet. The diagonalization of this matrix trivially gives two Weyl eigenstates of the same mass M_{St} , which can be assembled into a single massive Dirac fermion of the same mass. Notice that in this reidentification of the degrees of freedom contained

in $\hat{\mathbf{b}}$ and in the vector multiplet \hat{B} , $\text{Im}b$ takes the role of a Nambu-Goldstone mode and can be gauged away.

The saxion has typical interactions of the form $\text{Re}b F_i F_j$, with the gauge fields which have mixed anomalies with $U(1)_B$, beside nonpolynomial interactions with the remaining fields of the theory. As we are going to elaborate, this features shows up because of the presence of terms consisting of the product of two D fields and the saxion. To clarify this point, we recall that the general Lagrangian contains a supersymmetric Wess-Zumino term of the form

$$\mathcal{L}_{\text{WZ}Y} = -\frac{1}{2} \int d^4\theta \frac{c_Y}{M_{\text{St}}} \hat{\mathbf{b}} W_\alpha^Y W^{\alpha} \delta(\bar{\theta}^2) + \text{H.c.}, \quad (12)$$

which gives, after the expansion in components, a term proportional to

$$\frac{c_Y}{M_{\text{St}}} \text{Re}b D_Y D_Y. \quad (13)$$

This kind of terms, once the equations of motion (EOM) of the auxiliary fields D are calculated and substituted back into the Lagrangian, give the nonpolynomial form of the potential. Furthermore, from the WZ term corresponding to the anomaly BBY (which is the term proportional to c_{YB}), we get a term proportional to $\text{Re}b D_Y D_B$ so that the EOM for the Abelian D fields are coupled. The derivation of such equations involves all the terms of the Lagrangian discussed in Appendix A. We obtain

$$D_{B,\text{OS}} = \frac{1}{12 + 12\sqrt{2}\text{Re}b(c_B + c_Y)/M_{\text{St}} - 6\text{Re}b^2(c_{YB}^2 - 4c_Y c_B)/M_{\text{St}}^2} \left\{ \left[2 \frac{c_B}{M_{\text{St}}} \left(\sqrt{2} + 2 \frac{c_Y}{M_{\text{St}}} \text{Re}b \right) - \frac{c_{YB}^2}{M_{\text{St}}^2} \text{Re}b \right] (-3i\lambda_B \psi_{\mathbf{b}} + \text{H.c.}) \right. \\ - 12M_{\text{St}} \text{Re}b - 12\sqrt{2}c_Y \text{Re}b^2 + 12g_B \left(1 + \sqrt{2} \frac{c_Y}{M_{\text{St}}} \text{Re}b \right) (B_S S^\dagger S + B_{H_1} H_1^\dagger H_1 \\ + B_{H_2} H_2^\dagger H_2 + B_{D_R} \tilde{D}_R^\dagger \tilde{D}_R + B_{U_R} \tilde{U}_R^\dagger \tilde{U}_R + B_Q \tilde{Q}^\dagger \tilde{Q} + B_R \tilde{R}^\dagger \tilde{R} + B_L \tilde{L}^\dagger \tilde{L}) + 3\sqrt{2} \frac{c_{YB}}{M_{\text{St}}} (i\lambda_Y \psi_{\mathbf{b}} + \text{H.c.}) \\ \left. + \sqrt{2} \frac{c_{YB}}{M_{\text{St}}} g_Y \text{Re}b (-3H_1^\dagger H_1 + 3B_{H_2} H_2^\dagger H_2 + 2\tilde{D}_R^\dagger \tilde{D}_R - 4\tilde{U}_R^\dagger \tilde{U}_R + \tilde{Q}^\dagger \tilde{Q} + 6\tilde{R}^\dagger \tilde{R} - 3\tilde{L}^\dagger \tilde{L}) \right\}, \\ D_{Y,\text{OS}} = \frac{1}{12 + 12\sqrt{2}\text{Re}b(c_B + c_Y)/M_{\text{St}} - 6\text{Re}b^2(c_{YB}^2 - 4c_Y c_B)/M_{\text{St}}^2} \left\{ 3 \frac{c_{YB}^2}{M_{\text{St}}^2} \text{Re}b (i\lambda_Y \psi_{\mathbf{b}} + \text{H.c.}) + 3\sqrt{2} \frac{c_{YB}}{M_{\text{St}}} (i\lambda_Y \psi_{\mathbf{b}} + \text{H.c.}) \right. \\ - 6\sqrt{2}c_{YB} \text{Re}b^2 + 6\sqrt{2} \frac{c_{YB}}{M_{\text{St}}} \text{Re}b g_B (B_S S^\dagger S + B_{H_1} H_1^\dagger H_1 + B_{H_2} H_2^\dagger H_2 + B_{D_R} \tilde{D}_R^\dagger \tilde{D}_R + B_{U_R} \tilde{U}_R^\dagger \tilde{U}_R \\ \left. + 2g_B \left(1 + \sqrt{2} \frac{c_B}{M_{\text{St}}} \text{Re}b \right) (-3H_1^\dagger H_1 + 3B_{H_2} H_2^\dagger H_2 + 2\tilde{D}_R^\dagger \tilde{D}_R - 4\tilde{U}_R^\dagger \tilde{U}_R + \tilde{Q}^\dagger \tilde{Q} + 6\tilde{R}^\dagger \tilde{R} - 3\tilde{L}^\dagger \tilde{L}) \right\}, \quad (14)$$

showing that their on-shell expressions are characterized by the appearance of the saxion field in a nonpolynomial form. The presence of the Stückelberg mass allows one to perform an expansion of these terms to all orders in $\text{Re}b/M_{\text{St}}$. The first terms of the series expansion are given by

$$\frac{1}{12 + 12\sqrt{2}\text{Re}b(c_B + c_Y)/M_{\text{St}} - 6\text{Re}b^2(c_{YB}^2 - 4c_Y c_B)/M_{\text{St}}^2} \\ = \frac{1}{12} - c_Y \frac{\text{Re}b}{6\sqrt{2}M_{\text{St}}} - c_B \frac{\text{Re}b}{6\sqrt{2}M_{\text{St}}} + \frac{1}{6} c_Y^2 \frac{\text{Re}b^2}{M_{\text{St}}^2} + \frac{1}{24} c_{YB}^2 \frac{\text{Re}b^2}{M_{\text{St}}^2} + \frac{1}{6} c_B^2 \frac{\text{Re}b^2}{M_{\text{St}}^2} + \frac{1}{6} c_B c_Y \frac{\text{Re}b^2}{M_{\text{St}}^2} + O(\text{Re}b^2/M_{\text{St}}^2). \quad (15)$$

We present a list of the vertices to leading order in $1/M_{\text{St}}$ in Fig. 1. Additional vertices (not shown) come with n insertions of $\text{Re}b$ and a suppression by higher powers ($2n$) of M_{St} . Some considerations are in order concerning the allowed values of M_{St} . A very large Stückelberg mass, in principle, would be sufficient to guarantee that the effect of reheating—caused by the decay of the saxion—takes place well above the temperature of nucleosynthesis (see for instance the discussion in [32]) thereby avoiding the problem of a possible late entropy release at that time. In this case one can essentially neglect the saxion from the low energy spectrum. For moduli of string origin the required mass value (~ 100 TeV), much larger than in our case, is justified by the suppressed gravitational interaction of the modulus with

the rest of the matter fields and works as an enhancing factor for its decay. In our case, instead, such a suppression is absent and a fast decay of the saxion is guaranteed already by a Stückelberg mass around the TeV scale.

III. THE SCALAR POTENTIAL AND THE SAXION

As we have mentioned, in this model there are three scalar fields which take a VEV, H_1 , H_2 , and S , the scalar components of the scalar superfield \hat{S} . We assume that also the saxion field gets a VEV, v_b . The scalar potential is composed by contributions coming from the D terms, F terms, and scalar mass terms. Expanding up to $\mathcal{O}(\text{Re}b/M_{\text{St}})$ we find

$$\begin{aligned}
 V = & |\lambda H_1 \cdot H_2|^2 + |\lambda S|^2(|H_1|^2 + |H_2|^2) + m_1^2 |H_1|^2 + m_2^2 |H_2|^2 + m_S^2 |S|^2 + (a_\lambda S H_1 \cdot H_2 + \text{H.c.}) \\
 & - \frac{1}{8} g_Y^2 (H_1^\dagger H_1 - H_2^\dagger H_2)^2 - \frac{1}{2} g_B^2 (B_{H_1} H_1^\dagger H_1 + B_{H_2} H_2^\dagger H_2 + B_S S^\dagger S)^2 - \frac{1}{8} g_2^2 [(H_1^\dagger H_1 - H_2^\dagger H_2)^2 + 4|H_1^\dagger H_2|^2] \\
 & + \text{Re}b^3 \left[\frac{c_B M_{\text{St}}}{\sqrt{2}} + g_Y \frac{(c_Y + c_B) c_{YB}}{2M_{\text{St}}} (H_1^\dagger H_1 - H_2^\dagger H_2) \right] - \text{Re}b^2 \left[\frac{m_{\text{Re}b}^2}{2} + \frac{M_{\text{St}}^2}{2} + \sqrt{2} c_B g_B (B_{H_1} H_1^\dagger H_1 \right. \\
 & + B_{H_2} H_2^\dagger H_2 + B_S S^\dagger S) + \frac{c_{YB} g_B}{2\sqrt{2}} (H_1^\dagger H_1 - H_2^\dagger H_2) \left. \right] + \text{Re}b \left\{ g_B M_{\text{St}} (B_{H_1} H_1^\dagger H_1 + B_{H_2} H_2^\dagger H_2 + B_S S^\dagger S) \right. \\
 & + \frac{c_W g_2}{32\sqrt{2} M_{\text{St}}} [(H_1^\dagger H_1 - H_2^\dagger H_2)^2 + 4|H_1^\dagger H_2|^2] + \frac{c_Y g_Y^2}{4\sqrt{2} M_{\text{St}}} (H_1^\dagger H_1 - H_2^\dagger H_2)^2 + \frac{c_B g_B^2}{\sqrt{2} M_{\text{St}}} (B_{H_1} H_1^\dagger H_1 + B_{H_2} H_2^\dagger H_2 + B_S S^\dagger S)^2 \\
 & \left. + \frac{c_{YB} g_Y g_B}{2\sqrt{2} M_{\text{St}}} (B_{H_1} H_1^\dagger H_1 + B_{H_2} H_2^\dagger H_2 + B_S S^\dagger S) (H_1^\dagger H_1 - H_2^\dagger H_2) \right\}. \tag{16}
 \end{aligned}$$

To proceed with the analysis of this potential we introduce the following parametrizations:

$$\begin{aligned}
 H_1 &= \frac{1}{\sqrt{2}} \begin{pmatrix} \text{Re}H_1^0 + i \text{Im}H_1^0 \\ \text{Re}H_1^- + i \text{Im}H_1^- \end{pmatrix}, \\
 H_2 &= \frac{1}{\sqrt{2}} \begin{pmatrix} \text{Re}H_2^+ + i \text{Im}H_2^+ \\ \text{Re}H_2^0 + i \text{Im}H_2^0 \end{pmatrix}, \quad S = \frac{1}{\sqrt{2}} (\text{Re}S + i \text{Im}S),
 \end{aligned}$$

expanded around the VEVs of the Higgs fields and of the saxion as

$$\begin{aligned}
 \langle H_1 \rangle &= \frac{1}{\sqrt{2}} \begin{pmatrix} v_1 \\ 0 \end{pmatrix}, \quad \langle H_2 \rangle = \frac{1}{\sqrt{2}} \begin{pmatrix} 0 \\ v_2 \end{pmatrix}, \quad \tan\beta = \frac{v_2}{v_1}, \\
 \langle S \rangle &= \frac{v_S}{\sqrt{2}}, \quad \langle \text{Re}b \rangle = \frac{v_b}{\sqrt{2}}. \tag{17}
 \end{aligned}$$

The scalar mass parameters can be expressed in terms of the remaining parameters of the theory using the minimization conditions for the scalar potential. In particular, taking a derivative of the potential with respect to the saxion field we get the relation

$$\begin{aligned}
 \frac{\partial V}{\partial \text{Re}b} = & -v_b m_{\text{Re}b}^2 - v_b M_{\text{St}}^2 + \frac{1}{2} g_B M_{\text{St}} B_{H_1} v_1^2 \\
 & + \frac{1}{2} g_B M_{\text{St}} B_{H_2} v_2^2 + \frac{1}{2} g_B M_{\text{St}} B_S v_S^2, \tag{18}
 \end{aligned}$$

where we have neglected all the contributions suppressed by the Stückelberg mass. We can use this relation as a necessary condition in order to express $m_{\text{Re}b}^2$ in terms of the VEVs and of the other parameters of the scalar potential. A numerical analysis of the Hessian at this point, for the selected parameters of the model used in our simulations, shows that indeed this extremal point indeed corresponds to a minimum.

We will try to highlight the most interesting features of these types of models and the implications for the axion, which are all connected to the properties of the vacuum of these theories below the scale of SUSY breaking and at the scales of the electroweak and QCD phase transitions.

IV. SAXION DECAY MODES

Having summarized the basic structure of the model, we now turn to describe the leading contributions to the 2-body decays of the saxion. The goal of this analysis is to ensure that the decay rate of the saxion is such that it occurs fast enough in order not to interfere with the nucleosynthesis.

We will compute its decay rate by considering the worst possible scenario, i.e. by assuming that this decay occurs around the SUSY breaking scale, or temperature T around 1 TeV. At this temperature, the decays of the

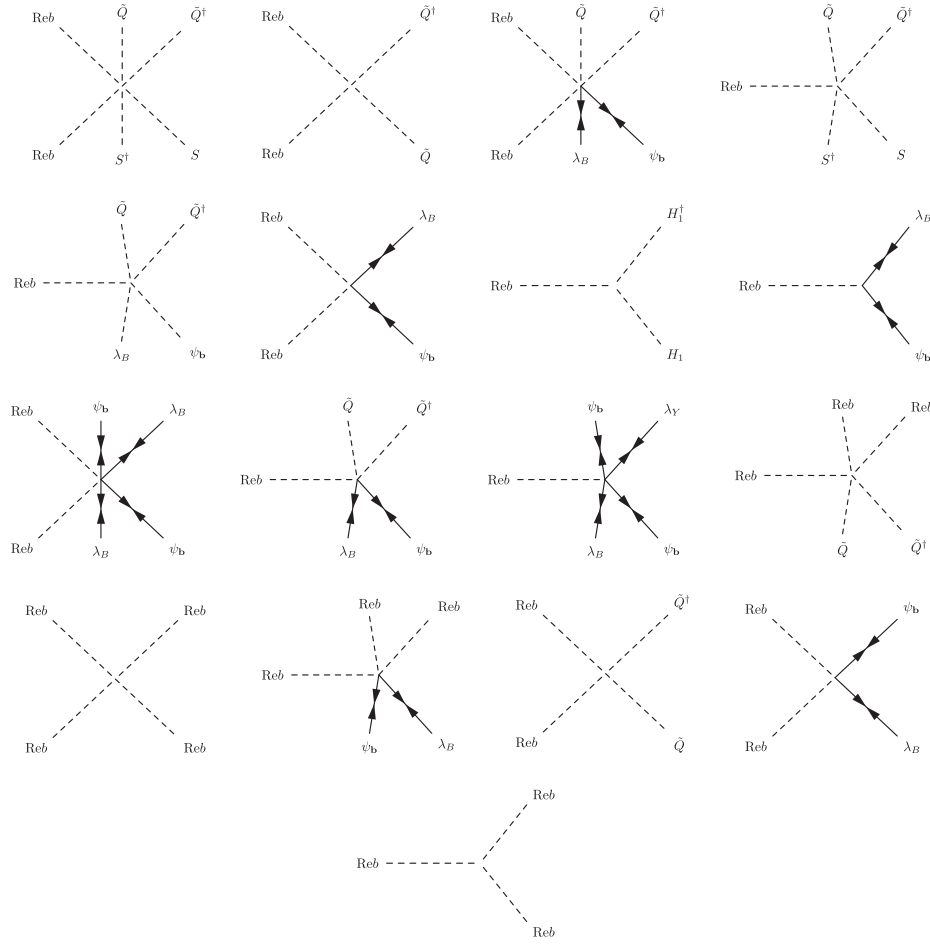


FIG. 1. Saxion interactions to lowest order in $1/M_{St}$. An infinite number of additional higher order interactions (in powers of $1/M_{St}$) are generated by the insertion on these vertices of n powers of saxion lines. We use the double line notation for Majorana particles.

saxion are parametrized by the typical SUSY breaking scales such as M_b and M_Y , both of $O(M_{SUSY})$. The model is in a symmetric electroweak phase ($M_{SUSY} > v$), which justifies the use of the interaction eigenstates (rather than

the mass eigenstates) for the description of the final decay products.

The relevant interactions for the saxion decay are described by the general Lagrangian

$$\begin{aligned}
 \mathcal{L}_{\text{saxion dec}} = \text{Reb} & \left[g_B M_{St} B_{H_1} H_1^\dagger H_1 + g_B M_{St} B_{H_2} H_2^\dagger H_2 + g_B M_{St} B_S S^\dagger S + g_B M_{St} B_Q \sum_{j=1}^3 \tilde{Q}_j^\dagger \tilde{Q}_j + g_B M_{St} B_{D_R} \sum_{j=1}^3 \tilde{D}_{R,j}^\dagger \tilde{D}_{R,j} \right. \\
 & + g_B M_{St} B_{U_R} \sum_{j=1}^3 \tilde{U}_{R,j}^\dagger \tilde{U}_{R,j} + g_B M_{St} B_L \sum_{l=e,\mu,\tau} \tilde{L}_l^\dagger \tilde{L}_l + g_B M_{St} B_R \sum_{l=e,\mu,\tau} \tilde{R}_l^\dagger \tilde{R}_l - i \frac{c_B}{2\sqrt{2}} (\lambda_B \psi_{\mathbf{b}} + \bar{\lambda}_B \bar{\psi}_{\mathbf{b}}) \\
 & \left. - i \frac{c_{YB}}{2\sqrt{2}} (\psi_{\mathbf{b}} \lambda_Y + \bar{\psi}_{\mathbf{b}} \bar{\lambda}_Y) \right]. \tag{19}
 \end{aligned}$$

They involve CP -even and CP -odd massless scalars, the extra singlet scalar S , the squarks, and the sleptons and the gauginos $\psi_{\mathbf{b}}$, λ_Y . We compute the total decay rate into fermions, squarks and sleptons, and Higgs scalars. The left-handed doublets of the squarks and the sleptons are defined as

\tilde{Q}_j and \tilde{L}_l , respectively, while the right-handed singlets are $\tilde{U}_{R,j}$, $\tilde{D}_{R,j}$, and \tilde{R}_l , with j, l labeling the fermion families.

(i) *Decays into fermions.*—Assuming that $M_{\mathbf{b}} \approx M_Y$ are slightly less than 1 TeV, the decay rates of the saxion into one gaugino and one axino are

$$\Gamma(\text{Re}b \rightarrow \bar{\lambda}_B \psi_{\mathbf{b}}) = c_B^2 \frac{M_{\text{Re}b}}{32\pi} \left(1 - 4 \frac{M_{\mathbf{b}}^2}{M_{\text{Re}b}^2}\right)^{3/2},$$

$$\Gamma(\text{Re}b \rightarrow \bar{\lambda}_Y \psi_{\mathbf{b}}) = c_{YB}^2 \frac{M_{\text{Re}b}}{32\pi} \left(1 - 4 \frac{M_Y^2}{M_{\text{Re}b}^2}\right)^{3/2} \quad (20)$$

with the expressions of the coefficients c_B and c_{YB} determining the couplings given explicitly in Eq. (4). Notice that these rates are large due to the linear dependence on $M_{\text{Re}b}$ ($= M_{\text{St}}$).

(ii) *Decays into squarks and sleptons.*—In this channel we consider, for simplicity, the decay only into squarks and sleptons of the same type. Even in this case we are assuming that the masses of the squarks and of the sleptons are all equal and slightly below 1 TeV. The decay rate into the i -type sfermion is given by

$$\Gamma(\text{Re}b \rightarrow \tilde{f}_i^\dagger \tilde{f}_i) = \frac{g_i^2 \lambda^{1/2}}{16\pi M_{\text{Re}b}^3}, \quad (21)$$

where the kinematic function λ is, in general, defined as $\lambda = (M_i^2 + M_j^2 - M_{\text{Re}b}^2)^2 - 4M_i^2 M_j^2$ (here with $M_i = M_j$), and the couplings g_i , in the various cases, are defined as

$$g_i = \begin{cases} N_c c_{U_R} & R\text{-handed singlet } u\text{-type squark,} \\ N_c c_{D_R} & R\text{-handed singlet } d\text{-type squark,} \\ N_c c_{Q_L} & L\text{-handed doublet squark,} \\ c_R & R\text{-handed singlet slepton } \tilde{e}, \tilde{\mu}, \tilde{\tau}, \\ c_L & L\text{-handed doublet slepton.} \end{cases} \quad (22)$$

Here $N_c = 3$ is the color factor and the various couplings are given as

$$\begin{aligned} c_{D_R} &= \frac{1}{2} g_B M_{\text{St}} B_{D_R}, & c_{U_R} &= \frac{1}{2} g_B M_{\text{St}} B_{U_R}, \\ c_{Q_L} &= -\frac{1}{2} g_B M_{\text{St}} B_Q, & c_L &= -\frac{1}{2} g_B M_{\text{St}} B_L, \\ c_R &= \frac{1}{2} g_B M_{\text{St}} B_R. \end{aligned} \quad (23)$$

(iii) *Decays into massless scalars.*—The decay rate into particles of the Higgs sector that we denote generically with $h_i = \text{Re}H_1, \text{Im}H_1, \dots$ is given by

$$\Gamma(\text{Re}b \rightarrow h_i h_i) = \frac{s_i^2}{32\pi M_{\text{Re}b}} \left(1 - 4 \frac{M_{s_i}^2}{M_{\text{Re}b}^2}\right)^{1/2}, \quad (24)$$

where the couplings s_i are defined as

$$s_i = \begin{cases} c_{H_1} & H_1 \text{ Higgs doublet,} \\ c_{H_2} & H_2 \text{ Higgs doublet,} \\ c_S & S \text{ Higgs singlet,} \end{cases} \quad (25)$$

and the coefficients c_{H_1} , c_{H_2} , and c_S are

$$\begin{aligned} c_{H_1} &= -\frac{1}{4} g_B M_{\text{St}} B_{H_1}, & c_{H_2} &= -\frac{1}{4} g_B M_{\text{St}} B_{H_2}, \\ c_S &= -\frac{1}{4} g_B M_{\text{St}} B_S. \end{aligned} \quad (26)$$

The total decay rate is obtained by summing over all the decay modes

$$\Gamma_{\text{tot}} = \Gamma(\text{Re}b \rightarrow \bar{\lambda}_b \psi_{\mathbf{b}}) + \Gamma(\text{Re}b \rightarrow \bar{\lambda}_Y \psi_{\mathbf{b}}) + \sum_i \Gamma(\text{Re}b \rightarrow \tilde{f}_i \tilde{f}_i) + \sum_i \Gamma(\text{Re}b \rightarrow h_i h_i). \quad (27)$$

All the decay rates depend upon the value of the extra $U_B(1)$ coupling g_B , the Stückelberg mass M_{St} , and the SUSY breaking scale M_{SUSY} .

The total decay rate and the lifetime of the saxion are shown in Fig. 2, with the saxion mass $M_{\text{Re}b}$ given by the Stückelberg scale ($M_{\text{Re}b} = M_{\text{St}}$) around 1.4 TeV, and with all the squarks and the sleptons in the final state taken of a

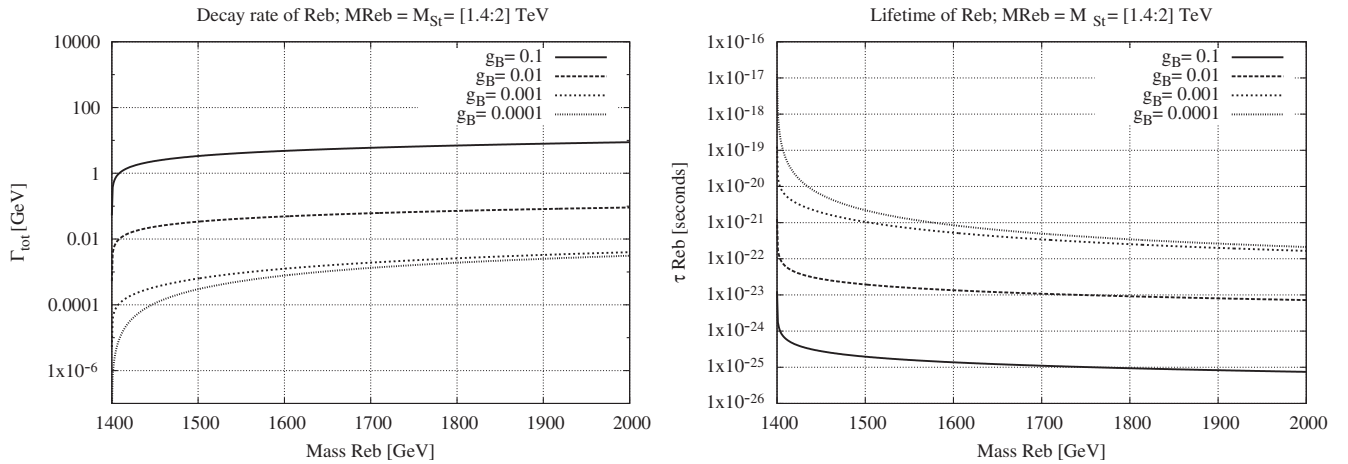


FIG. 2. Total decay rate and lifetime of the saxion for different values of g_B as a function of the Stückelberg mass.

mass of 700 GeV. All the particles of the Higgs sector are considered to be massless. For $g_B = 0.01$ we obtain a saxion whose decay rate is around 60 MeV if its mass is 1.7 TeV, and which decays rather quickly, since its lifetime is about 10^{-23} s. The lifetime decreases quite significantly as we increase the gauge coupling of the anomalous gauge symmetry. For instance, for $g_B = 0.1$ it decreases to $\sim 10^{-24}$ s, since the phase space for the decay is considerably enhanced.

We conclude that the saxion decays sufficiently fast and does not generate any late entropy release at the time of nucleosynthesis. Obviously, this scenario remains valid for all values of the Stückelberg mass above the 1 TeV value. Therefore, in the analysis of the evolution of the contributions to the total energy density (ρ) of the Universe, either due to matter (ρ_m) or to radiation (ρ_R), at temperatures $T \leq 2$ TeV, the contribution coming from the saxion is entirely accounted for by ρ_R .

At this point, having cleared the way of any possible obstruction due to the presence of moduli at the low energy stage ($T \leq 2$ TeV) of the evolution of our model, we are ready to discuss the relevant features of the Stückelberg field. In particular, we will discuss the appearance of a physical axion, the physical component of the Stückelberg, at the electroweak scale. This is extracted from the CP -odd sector and generated by the mechanism of vacuum misalignment taking place at the same scale. In particular, the discussion serves to illustrate how a flat—but physical—direction might be singled out from the vacuum manifold, acquiring a small curvature at the electroweak phase transition.

V. THE FLAT DIRECTION OF THE PHYSICAL AXION FROM HIGGS-AXION MIXING

In [34,35] we have presented in some detail an approximate procedure in order to identify in the CP -odd sector one state that inherits axionlike interactions. The approach did not require the explicit expressions of the curvature terms in the CP -odd part of the supersymmetric potential, which are instead needed in the discussion of the angle of misalignment. Here we are going to extend this analysis by giving the explicit parametrization of these additional terms. The determination of the angle of misalignment and its parametrization in terms of the physical axion is based on an extension of the method presented in [30]. We are going to illustrate this point starting, for simplicity, from the nonsupersymmetric case and then moving to the supersymmetric one.

A. The nonsupersymmetric case

In the nonsupersymmetric case the scalar sector contains two Higgs doublets $V_{PQ}(H_u, H_d)$ plus one extra contribution (a PQ breaking potential), denoted as $V_{\not{PQ}}(H_u, H_d, b)$, which mixes the Higgs sector with the Stückelberg axion b ,

$$V = V_{PQ}(H_u, H_d) + V_{\not{PQ}}(H_u, H_d, b). \quad (28)$$

The mixing induced in the CP -odd sector determines the presence of a linear combination of the Stückelberg field b and of the Goldstones of the CP -odd sector, called χ , which is characterized by an almost flat direction, whose curvature is controlled by the strength of the extra potential $V_{\not{PQ}}$. $V_{PQ}(H_u, H_d)$ is the ordinary potential of 2 Higgs doublets,

$$\begin{aligned} V_{PQ} = & \mu_u^2 H_u^\dagger H_u + \mu_d^2 H_d^\dagger H_d + \lambda_{uu}(H_u^\dagger H_u)^2 \\ & + \lambda_{dd}(H_d^\dagger H_d)^2 - 2\lambda_{ud}(H_u^\dagger H_u)(H_d^\dagger H_d) \\ & + 2\lambda'_{ud}|H_u^T \tau_2 H_d|^2. \end{aligned} \quad (29)$$

Concerning the $V_{\not{PQ}}$ contribution to the total potential, its structure is inferred on the basis of gauge invariance and given by

$$\begin{aligned} V_{\not{PQ}} = & \lambda_0(H_2^\dagger H_1 e^{-ig_B(B_{H_2} - B_{H_1})(b/2M_{St})}) \\ & + \lambda_1(H_2^\dagger H_1 e^{-ig_B(B_{H_2} - B_{H_1})(b/2M_{St})})^2 \\ & + \lambda_2(H_2^\dagger H_2)(H_2^\dagger H_1 e^{-ig_B(B_{H_2} - B_{H_1})(b/2M_{St})}) \\ & + \lambda_3(H_1^\dagger H_1)(H_2^\dagger H_1 e^{-ig_B(B_{H_2} - B_{H_1})(b/2M_{St})}) + \text{H.c.} \end{aligned} \quad (30)$$

These terms are the only ones allowed by the symmetry of the model and are parametrized by one dimensionful ($\lambda_0 \equiv \bar{\lambda}_0 v$) and three dimensionless constants ($\lambda_1, \lambda_2, \lambda_3$).

The CP -odd sector is then spanned by the three fields ($\text{Im}H_1, \text{Im}H_2$, and b), with the potential V_{PQ} a function only of H_1 and H_2 . After electroweak symmetry breaking, due to Higgs-axion mixing, b can be written as a linear combination of a physical axion and of an extra component. The latter is a linear combination of the two Goldstone modes of the total potential ($V_{PQ} + V_{\not{PQ}}$), denoted as G_0^1, G_0^2 . The physical axion, χ , i.e. the component of b which is not proportional to the two Goldstones, can be identified using the rotation matrix O^χ which relates interaction and mass eigenstates in the CP -odd sector

$$\begin{pmatrix} G_0^1 \\ G_0^2 \\ \chi \end{pmatrix} = O^\chi \begin{pmatrix} \text{Im}H_1^0 \\ \text{Im}H_2^0 \\ b \end{pmatrix}, \quad (31)$$

which takes the form

$$b = O_{13}^\chi G_0^1 + O_{23}^\chi G_0^2 + O_{33}^\chi \chi. \quad (32)$$

χ inherits WZ interactions from b via Eq. (32), once this is introduced into the WZ counterterms.

From an explicit computation one finds that $O_{13}^\chi = 0$, $O_{23}^\chi \sim O(1)$, and $O_{33}^\chi \sim v/M_{St}$. The Goldstones of the two neutral gauge bosons, $G_Z, G_{Z'}$ are linear combinations of G_0^1 and G_0^2 and can be extracted from the bilinear mixings after an expansion around the broken electroweak vacuum. Then, the entire CP -odd sector can be spanned by the basis

$(G_Z, G_{Z'}, \chi)$. The presence of an extra degree of freedom in this sector has been established in [33] using a simple counting of the degrees of freedom. We review this point for clarity.

There are 9 degrees of freedom in the set $(A_Y, W_3, B, \text{Im}H_1, \text{Im}H_2)$, where B is the massive Stückelberg gauge vector field, before electroweak symmetry breaking, as well as 9 in the set (A_Y, Z, Z', χ) , which is generated after the breaking. The direction determining the gauged axion χ is then physical but flat, in the absence of an extra potential which may depend explicitly on b . The potential V' is responsible for giving a small mass for χ and can be used to parametrize the mechanism of vacuum misalignment originated at the electroweak scale.

One can explore the structure of this potential and, in particular, investigate its periodicity. The phase of the potential is indeed parametrized by the ratio χ/σ_χ [30]

$$V_{\neq 0} = 4v_1v_2(\lambda_2v_1^2 + \lambda_3v_2^2 + \lambda_0)\cos\left(\frac{\chi}{\sigma_\chi}\right) + 2\lambda_1v_1^2v_2^2\cos\left(2\frac{\chi}{\sigma_\chi}\right) \quad (33)$$

with a mass for the physical axion χ given by

$$m_\chi^2 = \frac{2v_1v_2}{\sigma_\chi^2}(\bar{\lambda}_0v^2 + \lambda_2v_1^2 + \lambda_3v_2^2 + 4\lambda_1v_1v_2) \approx \lambda_{\text{eff}}v^2, \quad (34)$$

with $\sigma_\chi \sim O(v)$. The size of this expression is the result of two factors which appear in Eq. (34): the size of the potential, parametrized by $(\bar{\lambda}_0, \lambda_1, \lambda_2, \lambda_3)$, and the electroweak VEVs of the two Higgses. The appearance of χ in Eq. (33)—in the phase of the extra potential—shows explicitly that the angle of misalignment is entirely described by this field. The angle is defined as

$$\theta(x) \equiv \frac{\chi(x)}{\sigma_\chi}, \quad (35)$$

where

$$\sigma_\chi \equiv \frac{2v_1v_2M_{\text{St}}}{\sqrt{g_B^2(B_{H_2} - B_{H_1})^2v_1^2v_2^2 + 2M_{\text{St}}^2(v_1^2 + v_2^2)}} \quad (36)$$

is the new dimensionful constant which takes the same role of the scale f_a of the PQ case [$\theta(x) = a/f_a$]. The potential is characterized by a small strength $\sim \lambda_{\text{eff}}v^4$, and for this reason one can think of χ as a pseudo Nambu-Goldstone mode of the theory.

At this stage, it is important to realize that the size of the extra potential is significant in order to establish whether the degree of freedom associated with the axion field remains frozen or not at the electroweak scale. For instance, if λ_{eff} is associated with electroweak instantons ($\lambda_{\text{eff}} \sim \lambda_{\text{inst}}$), then m_χ is very suppressed (see the discussion in Sec. V C) and far smaller than the corresponding Hubble rate at the electroweak scale

$$H(T) = \frac{1}{3}\sqrt{\frac{4}{5}}\pi^3g_{*,T}\frac{T^2}{M_P}, \quad (37)$$

which is about 10^{-5} eV. In the expression above g_{*,T_i} is the number of effective massless degrees of freedom of the model at a given temperature (T), while M_P denotes the Planck mass. We recall that the condition

$$m_\chi(T) \sim 3H(T) \quad (38)$$

which ensures the presence of oscillations and determines implicitly the oscillation temperature T_i , is indeed impossible to satisfy if the misalignment that generates the value of m_χ at the electroweak scale is assumed of being of instanton origin (see the discussion in Appendix C). This implies that the degree of freedom associated with this physical axion would be essentially frozen at the electroweak scale, and the oscillations could take place at a later stage in the early universe, only around the QCD hadron transition. Instead, a more sizable potential, providing an axion mass larger than 10^{-5} eV, would allow such oscillations. For an axion mass around 1 MeV oscillations indeed occur, but are damped by the particle decay, given that its lifetime ($\tau_l \sim 10^{-4}$ s) is much larger than the period of their oscillation ($\tau_{\text{osc}} \sim 10^{-13}$ s). This discussion is going to be expanded to the supersymmetric case.

B. Supersymmetry and the angle of misalignment

In the supersymmetric case the situation is analogous, in the sense that the physical direction χ can be identified by the same criteria. The superpotential that we are considering allows the presence of 1 extra degree of freedom, given by $\text{Im}S$, to appear in the CP -odd sector beside the states $(\text{Im}H_1, \text{Im}H_2, \text{Im}b)$, already present in the nonsupersymmetric case.

From the supersymmetric potential V in (16), we identify two massless states that we call G_1^0 and G_2^0 , and a massive eigenstate, called H_4^0 . G_1^0 and G_2^0 do not coincide with the true Goldstones of the model, as in the previous case, since the V potential does not include any contribution involving $\text{Im}b$. The correct neutral Goldstone modes are extracted from the derivative couplings between the CP -odd scalar fields and the neutral gauge bosons present in the Lagrangian. The physical axion is then identified as the massless direction which is orthogonal to the subspace spanned by $(G_Z, G_{Z'}, H_4^0)$. This state is called $H_0^5 \equiv \chi$ and is given by the linear combination

$$\begin{aligned} \chi = \frac{1}{N_\chi} & [M_{\text{St}}v_1v_2^2\text{Im}H_1^0 + M_{\text{St}}v_1^2v_2\text{Im}H_2^0 \\ & - M_{\text{St}}v^2v_S\text{Im}S - B_Sg_B(v^2v_S^2 + v_1^2v_2^2)\text{Im}b], \\ N_\chi = \sqrt{M_{\text{St}}^2v^2(v^2v_S^2 + v_1^2v_2^2) + B_S^2g_B^2(v^2v_S^2 + v_1^2v_2^2)^2}. \end{aligned} \quad (39)$$

It is important to remark that this state is not constructed, at least at this stage, from the matrix O^χ , since the projection

of $\text{Im}b$ on χ would be zero, if the matrix O_χ were derived from the potential V since it does not depend on $\text{Im}b$. Also in this case, the identification of the Goldstones of the two neutral massive gauge bosons (Z and Z') is obtained by looking at the bilinear mixing terms; these appear in the Lagrangian once this is rewritten in the physical basis (in the form $M_Z Z \partial G_Z$, and $M_{Z'} Z' \partial G_{Z'}$). Then one can immediately figure out that the linear basis spanning the entire CP -odd sector can be completed by the addition of an extra, orthogonal state χ ($G_Z, G_{Z'}, H_4^0, \chi$). The new entry parametrizes a massless but physical direction in this sector. Once $\text{Im}b$ is reexpressed in terms of the physical axion χ and of the Goldstone modes $G_Z, G_{Z'}$ of the massive gauge bosons, χ will inherit from $\text{Im}b$ axionlike interactions and will be promoted to a generalized PQ axion.

At this point, having identified this flat but physical direction of the potential in the CP -odd sector, one can ask the obvious question whether the same potential can acquire a curvature. These effects are indeed parametrized by the strength (λ_{eff}) of the potential V' (the “extra potential”) that we are going to identify below, and which remains a free parameter in the theory.

One special comment is deserved by v_S , the VEV of the scalar singlet, which is new compared to the standard MSSM scenario and which is part of the scalar potential.

We recall that this new scale is essentially bound by the condition $\lambda v_S \sim \mu \sim 10^2\text{--}10^3$ GeV [see Eq. (A6)]. This defines the typical range for the μ term, which sets the scale of the interaction for the two Higgs doublets in supersymmetric theories.

In our case we are allowed to parametrize this new nonperturbative contribution (V') to the potential, as discussed in the previous section, in a rather straightforward way, by classifying all the phase-dependent operators which can be constructed using the fundamental fields of the model. In analogy to the nonsupersymmetric case (the MLSOM) [33] we rely only on gauge invariance as a guiding principle to identify them. These include, in particular, a dependence of V' , again in the form of a phase factor, from the Stückelberg field $\text{Im}b$.

The contributions appearing in V' do not need to be given necessarily in a supersymmetric form, since we are assuming that supersymmetry is already broken at the scale at which they appear ($v < M_{\text{SUSY}}$). They are parametrized in the form

$$V' = \sum_{i=1}^6 V_i, \quad (40)$$

where

$$\begin{aligned} V_1 &= a_1 S^4 e^{-i4g_B B_S (\text{Im}b/2M_{\text{St}})} + \text{H.c.}, \\ V_2 &= e^{-ig_B B_S (\text{Im}b/2M_{\text{St}})} (a_2 H_1 \cdot H_2 S^2 + b_2 H_1^\dagger H_1 S + b_3 H_2^\dagger H_2 S + b_4 S^\dagger S^2 + d_1 S) + \text{H.c.}, \\ V_3 &= e^{-ig_B 2B_S (\text{Im}b/2M_{\text{St}})} (a_3 H_1^\dagger H_1 S^2 + a_4 H_2^\dagger H_2 S^2 + a_5 S^\dagger S^3 + c_1 S^2) + \text{H.c.}, \\ V_4 &= a_6 (H_1 \cdot H_2)^2 e^{ig_B 2B_S (\text{Im}b/2M_{\text{St}})} + \text{H.c.}, \\ V_5 &= b_1 S^3 e^{-ig_B 3B_S (\text{Im}b/2M_{\text{St}})} + \text{H.c.}, \\ V_6 &= c_2 H_1 \cdot H_2 e^{ig_B B_S (\text{Im}b/2M_{\text{St}})} + \text{H.c.} \end{aligned} \quad (41)$$

In the expressions above we have grouped together terms that share the same phase factor. Notice that the parameters a_i, b_j, c_k , and d_1 carry different mass dimensions. For these reasons they can be parametrized by suitable powers of the SUSY breaking mass M_{SUSY} times λ_{eff} . We explicitly obtain the estimates

$$\begin{aligned} a_i &\sim \lambda_{\text{eff}}, & b_j &\sim \lambda_{\text{eff}} M_{\text{SUSY}}, & c_k &\sim \lambda_{\text{eff}} M_{\text{SUSY}}^2, \\ d_1 &\sim \lambda_{\text{eff}} M_{\text{SUSY}}^3. \end{aligned} \quad (42)$$

If we introduce any of the terms in Eq. (41), and recompute the CP -odd mass matrix using the new potential ($V + V'$), this gets modified, but we still find two massless eigenstates corresponding to the neutral Goldstone modes, which also in this case we call G_0^1 and G_0^2 . They can be expressed as linear combinations of the neutral Goldstone states coming from the derivative couplings between the gauge bosons and the CP -odd Higgs fields. An important point to make is that these states (Goldstone modes) do not depend on the parameters of the Peccei-Quinn breaking

potential, as we expect, since the presence of this extra potential does not affect the bilinear derivative couplings through which they are identified.

In the basis ($\text{Im}H_1^1, \text{Im}H_2^2, \text{Im}S, \text{Im}b$) they are given by

$$\begin{aligned} G_0^1 &= \left\{ \frac{v_1}{v}, \frac{-v_2}{v}, 0, 0 \right\}, \\ G_0^2 &= \frac{1}{\sqrt{M_{\text{St}}^2 + g_B^2 (B_{H_1}^2 v_1^2 + B_{H_2}^2 v_2^2 + B_S^2 v_S^2)}} \\ &\quad \times \left\{ g_B B_S \frac{v_1 v_2^2}{v^2}, g_B B_S \frac{v_1^2 v_2}{v^2}, -g_B B_S v_S, M_{\text{St}} \right\}. \end{aligned} \quad (43)$$

C. The strength of the potential and λ_{eff}

One important comment concerns the possible size of the axion mass m_χ induced by V' at the electroweak scale. In this respect we will take into account two basic possibilities. A first possibility that we will explore is to assume

that the axion mass is PQ like, in the milli-eV region; as a second possibility we will select an axion mass around the MeV region. These choices cover a region of parameter space that has never been analyzed in these types of models, while a study of the GeV region for the axion mass has been addressed before in [41]. These choices have to be confronted with constraints coming from (a) direct axion searches, (b) nucleosynthesis constraints, and (c) constraints on the relic densities from WMAP data.

A PQ-like axion is bound to emerge in the spectrum of the theory if the potential V' is strongly suppressed and the real mechanism of misalignment which determines its mass is the one taking place at the QCD transition, as illustrated in Fig. 3. The value of λ_{eff} , under these assumptions, should be truly small and one way to achieve this would be to attribute its origin to electroweak instantons. Using the numerical relations for the electromagnetic (α) and weak couplings (α_W), $1/\alpha(M_Z) = 128$ and $\alpha_W = \alpha/\sin^2\theta_W$ with $\sin^2\theta_W(M_Z) = 0.23$ on the Z mass ($\alpha_W(M_Z) = 0.034$), the exponential suppression of the extra potential is controlled by $\lambda_{\text{eff}} \sim e^{-185} \equiv \lambda_{\text{inst}} = 4.5 \times 10^{-81}$. This corresponds to a mass for the axion given by $m_\chi \sim \sqrt{\lambda_{\text{eff}}} v \sim 10^{-29}$ eV. This mass would be obviously redefined at the QCD epoch.

As we have briefly mentioned in the Introduction, mass values of the axion field around 10^{-33} eV [for global U(1)'s or of PQ type] and with a spontaneous breaking scale $f_a \sim 10^{18}$ eV have been considered as a possible origin of a cosmological constant $\Lambda^4 \sim (10^{-3} \text{ eV})^4$ [11]. In such models the misalignment is purely of electroweak origin and connected to electroweak instantons. Oscillations of fields of such a mass would not take place even at the current cosmological time.

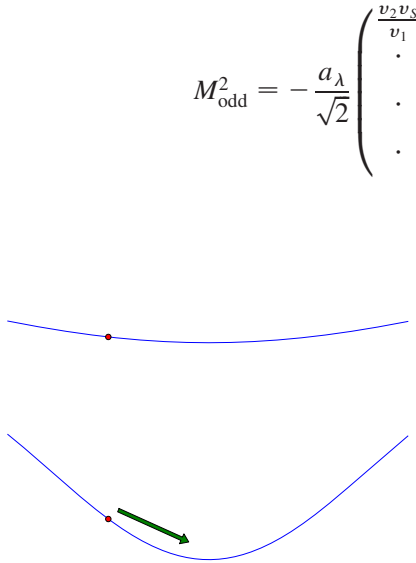


FIG. 3 (color online). Illustration of the two misalignments at the electroweak (upper curve) and at the QCD phase transitions (lower curve) for a PQ-like axion (not to scale).

Instead, for an axion of a mass in the MeV region, the value of λ_{eff} is larger ($\sim 10^{-12}$) and will be estimated below. In this case the effect of vacuum misalignment at the QCD scale is irrelevant in determining the mass of this particle. A more massive axion, in fact, decays at a much faster rate than a very light one and the usual picture typical of a long-lived PQ-like axion, in this specific case, simply does not apply.

In order to characterize in more detail the potential in Eq. (40), we proceed with a careful analysis of the field dependence of the phase factors in the exponentials that we expect to be written exclusively in terms of the physical fields of the CP -odd sector, H_0^4 , and the axion χ ($\chi \equiv H_0^5$). In fact, this is the analogous (and a generalization) of what was found in the previous section [see Eq. (33)], where the periodicity has been shown to depend only on the axion χ . For this purpose we use the following parametrization of the fields:

$$\begin{aligned} H_1^1(x) &= \frac{1}{\sqrt{2}}(\rho_1^1(x) + v_1)e^{i\Phi_1^1(x)}, \\ H_1^2(x) &= \frac{1}{\sqrt{2}}\rho_1^2(x)e^{i\Phi_1^2(x)}, & H_2^1(x) &= \frac{1}{\sqrt{2}}\rho_2^1(x)e^{i\Phi_2^1(x)}, \\ H_2^2(x) &= \frac{1}{\sqrt{2}}(\rho_2^2(x) + v_2), & e^{i\Phi_2^2(x)} \\ S(x) &= \frac{1}{\sqrt{2}}(\rho_S(x) + v_S)e^{i\Phi_S(x)}, \end{aligned} \quad (44)$$

and select some of the V_i in Eq. (41) in order to illustrate the general behavior.

For instance, if we consider only the V_1 term we get the corresponding symmetric mass matrix for the total potential $V + V_1$, with V defined in Eq. (16),

$$M_{\text{odd}}^2 = -\frac{a_\lambda}{\sqrt{2}} \begin{pmatrix} \frac{v_2 v_S}{v_1} & v_S & v_2 & 0 \\ \cdot & \frac{v_1 v_S}{v_2} & v_1 & 0 \\ \cdot & \cdot & \frac{v_1 v_2}{v_S} + 8\sqrt{2}\frac{a_1}{a_\lambda} v_S^2 & -4\sqrt{2}\frac{a_1}{a_\lambda} \frac{g_B B_S v_S^3}{M_{\text{St}}} \\ \cdot & \cdot & \cdot & 2\sqrt{2}\frac{a_1}{a_\lambda} \frac{g_B^2 B_S^2 v_S^4}{M_{\text{St}}^2} \end{pmatrix}, \quad (45)$$

expressed in the basis $(\Phi_1^1, \Phi_2^2, \Phi_S, \text{Im}b)$. From this matrix we get two null eigenvalues corresponding to the neutral Goldstones and two eigenvalues which correspond to the masses of the two CP -odd states H_0^4 and H_0^5 . In this specific case they take the form

$$\begin{aligned} m_{H_0^4, H_0^5}^2 &= \frac{1}{2M_{\text{St}} v_1 v_2 v_S} (A \pm \sqrt{A^2 - B}), \\ A &= 4a_1 v_1 v_2 v_S^3 (4M_{\text{St}}^2 + g_B^2 B_S^2 v_S^2) \\ &\quad + \sqrt{2} a_\lambda M_{\text{St}}^2 (v_1^2 v_2^2 + v^2 v_S^2), \\ B &= 16\sqrt{2} a_1 a_\lambda M_{\text{St}}^2 v_1 v_2 v_S^5 (4v^2 M_{\text{St}}^2 \\ &\quad + g_B^2 B_S^2 (v_1^2 v_2^2 + v^2 v_S^2)). \end{aligned} \quad (46)$$

In the limit of a vanishing a_1 ($\sim \lambda_{\text{eff}}$) we obtain a massless state corresponding to $H_0^5(\chi)$ and a massive one corresponding to H_0^4 . In fact, expanding the expressions above up to first order in a_1 , which is a very small parameter due to (42), we obtain for the two eigenvalues the approximate forms

$$m_{H_0^4}^2 \simeq \sqrt{2}a_\lambda \left(\frac{v_1 v_2}{v_S} + \frac{v_1 v_S}{v_2} + \frac{v_2 v_S}{v_1} \right) + 16a_1 \frac{v_1^2 v_2^2 v_S^2}{v^2 v_S^2 + v_1^2 v_2^2},$$

$$m_{H_0^5}^2 \simeq \frac{4a_1 v_S^4 [4v^2 M_{\text{St}}^2 + g_B^2 B_S^2 (v^2 v_S^2 + v_1^2 v_2^2)]}{M_{\text{St}}^2 (v^2 v_S^2 + v_1^2 v_2^2)}. \quad (47)$$

These relations show that indeed $m_{H_0^5}$ is $O(\lambda_{\text{eff}} v)$ while $m_{H_0^4}$ is $O(v)$.

Moving to the analysis of the phase factor of the same term (V_1), the linear combination of fields that appears in the exponential factor is given by the expression

$$\bar{\theta}_1 \equiv \frac{4\Phi_S(x)}{v_S} - \frac{2g_B B_S \text{Im}b(x)}{M_{\text{St}}}. \quad (48)$$

We rotate this linear combination on the physical basis (G_Z, G_Z, H_0^4, H_0^5) using the rotation matrix O^χ . After the rotation we can reexpress the angle of misalignment as a linear combination of the physical states of the CP -odd sector in the form

$$\bar{\theta}_1 = \frac{H_0^4}{\sigma_{H_0^4}} + \frac{H_0^5}{\sigma_{H_0^5}}. \quad (49)$$

This linear combination will appear in all the operatorial terms included in V' and is a generalization of Eq. (35), with $\sigma_{H_0^4}$ and $\sigma_{H_0^5}$ defining, separately, the scales of the two angular contributions to the total phase. It is not difficult to show that the periodicity of the potential depends predominantly on H_0^4 . This can be easily seen by analyzing the size of $\sigma_{H_0^4}$ and $\sigma_{H_0^5}$. In fact, expanding to first order in a_1 we get

$$\frac{1}{\sigma_{H_0^4}} = -\frac{4v_1 v_2}{v_2 \text{sgn} B_S \sqrt{v^2 v_S^2 + v_1^2 v_2^2}} - \frac{8\sqrt{2}v_1^2 v_2^2 v_S^4 [4v^2 M_{\text{St}}^2 + g_B^2 B_S^2 (v^2 v_S^2 + v_1^2 v_2^2)] a_1}{a_\lambda M_{\text{St}}^2 (v^2 v_S^2 + v_1^2 v_2^2)^{5/2} \text{sgn}(B_S)} + O(a_1^2),$$

$$\frac{1}{\sigma_{H_0^5}} = -\frac{8\sqrt{2}v_1^2 v_2^2 v_S^4 [4v^2 M_{\text{St}}^2 + g_B^2 B_S^2 (v^2 v_S^2 + v_1^2 v_2^2)] a_1}{a_\lambda M_{\text{St}}^2 (v^2 v_S^2 + v_1^2 v_2^2)^{5/2} \text{sgn} B_S} + O(a_1^2), \quad (50)$$

with a_λ being proportional to the SUSY breaking scale M_{SUSY} . A more careful look at the structure of these two scales shows that $\sigma_{H_0^4} \sim v_S$ ($v_S = 400$ GeV in our case) while $\sigma_{H_0^5} \sim M_{\text{SUSY}}/\lambda_{\text{eff}}$. Clearly, $\sigma_{H_0^5} \gg \sigma_{H_0^4}$, but the dependence of the extra potential on χ is clearly affected by the different possible sizes of λ_{eff} . For an instanton generated potential ($\lambda_{\text{eff}} \sim \lambda_{\text{inst}}$) the direction of χ is essentially flat and $\sigma_{H_0^5}$ turns out to be very large. In turn, this implies that the dependence of the potential V_1 on H_0^5 , which takes place exclusively through the exponential, is negligible, being essentially controlled by H_0^4 ($\bar{\theta}_1 \sim H_0^4/v$) with

$$V_1 \sim \lambda_{\text{eff}} v^4 \cos(\bar{\theta}_1). \quad (51)$$

We can conclude, indeed, that in this case the effect of misalignment on χ , generated at the electroweak scale, can be neglected. This feature is shown in the left panel of Fig. 4, where we plot $V'(H_0^4, \chi)$. It is immediately clear from these plots that for $\lambda_{\text{eff}} \sim \lambda_{\text{inst}}$ the only periodicity of the extra potential is in the variable H_0^4 (left panel), due to the flatness of the H_0^5 direction. For a more sizable potential, with $\lambda_{\text{eff}} \sim 10^{-12}$, the curvature generated in χ is responsible for giving a mass to the axion in the MeV range (Fig. 4, right panel). This result is generic for all the terms. One can draw some conclusions regarding the role played by the exponential phase and compare the supersymmetric with the nonsupersymmetric case. In the nonsupersymmetric case the periodicity of the potential is controlled by the weak scale (v) and is expressed directly

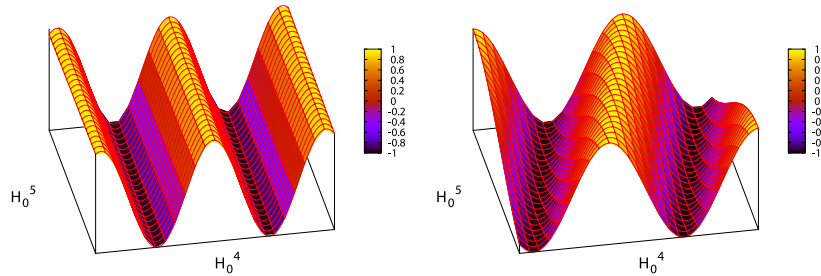


FIG. 4 (color online). Shape of the extra potential V' at the electroweak scale in the CP -odd sector in the $(H_0^4, \chi \equiv H_0^5)$ plane. χ is an almost flat direction for a strength induced by the instanton vacuum at the electroweak scale (left panel) and acquires a curvature for an axion mass in the MeV region (curvature in the χ direction, right panel).

in terms of the physical component of b (which is a real field). The size of the potential, in this case, is of order $\lambda_{\text{eff}} v^4$

$$V' \sim \lambda_{\text{eff}} v^4 \cos\left(\frac{\chi}{v}\right) \quad (52)$$

and therefore very small, while the periodicity shows that the amplitude of the axion field is $\chi \sim O(v)$. In the supersymmetric case, more generally, we obtain for a generic component V_i

$$V' \sim \lambda M_{\text{SUSY}}^4 \cos\left(\frac{H_0^4}{v_S} + \frac{\chi}{M_{\text{SUSY}}/\lambda_{\text{eff}}}\right) \quad (53)$$

from which it is clear that the curvature in the axion field is controlled by the parameter λ_{eff} . In the supersymmetric case we can think of the periodicity in Eq. (53) as essentially controlled by the massive CP -odd Higgs H_0^4 , with a period which is $O(\pi v_S)$, with superimposed a second periodicity of $O(\pi M_{\text{SUSY}}/\lambda_{\text{eff}})$ (with $M_{\text{SUSY}}/\lambda_{\text{eff}} \gg v_S$) in the perpendicular direction (χ). We conclude that the actual structure of the complete ($V + V'$) potential indeed guarantees the presence in the spectrum of a physical and light pseudoscalar field. This analysis holds, in principle, for an axion of any mass, although we do not explicitly study an axion whose mass goes beyond the MeV region. To have an axion which is long lived, the true discriminant of our study is the axion mass, and for this reason we are going to present a study of the decay rates of this particle keeping the mass as a free parameter varying in the milli-eV–MeV interval.

VI. DECAY OF A GAUGED SUPERSYMMETRIC AXION

In this section we compute the decay rate of the axion of the supersymmetric model into two photons, mediated both by the direct PQ interaction and by the fermion loop, which are shown in Fig. 5, keeping the axion mass as a free parameter. Denoting with $N_c(f)$ the color factor for a fermion specie, and introducing the function $\tau_f \eta(\tau_f)$, a function of the mass of the fermions circulating in the loop with

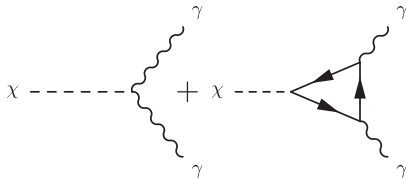


FIG. 5. Contributions to the axi-Higgs decay $\chi \rightarrow \gamma\gamma$.

$$\tau = 4m_f^2/m_\chi^2, \quad \eta(\tau) = \arctan^2 \frac{1}{\sqrt{-\rho_{f\chi}^2}}, \quad (54)$$

$$\rho_{f\chi} = \sqrt{1 - \left(\frac{2m_f}{m_\chi}\right)^2},$$

the WZ interaction in Fig. 5 is given by

$$\mathcal{M}_{\text{WZ}}^{\mu\nu}(\chi \rightarrow \gamma\gamma) = 4g_{\gamma\gamma}^\chi \varepsilon[\mu, \nu, k_1, k_2], \quad (55)$$

where $g_{\gamma\gamma}^\chi$ is the coupling, defined via the relations

$$g_{\gamma\gamma}^\chi = -\frac{g_B B_S (4c_Y g_2^2 + c_W g_Y^2)}{16g^2 M_{\text{St}}} \times \sqrt{\frac{v^2 v_S^2 + v_1^2 v_2^2}{4M_{\text{St}}^2 v^2 + g_B^2 B_S^2 (v^2 v_S^2 + v_1^2 v_2^2)}} \quad (56)$$

obtained from the rotation of the WZ vertices on the physical basis (we will comment in more detail on the size of this coupling in the next section). The massless contribution to the decay rate coming from the WZ counterterm $\chi F_\gamma F_\gamma$ is given by

$$\Gamma_{\text{WZ}}(\chi \rightarrow \gamma\gamma) = \frac{m_\chi^3}{4\pi} (g_{\gamma\gamma}^\chi)^2. \quad (57)$$

Combining also in this case the tree-level decay with the 1-loop amplitude, we obtain for $\chi \rightarrow \gamma\gamma$ the amplitude

$$\mathcal{M}^{\mu\nu}(\chi \rightarrow \gamma\gamma) = \mathcal{M}_{\text{WZ}}^{\mu\nu} + \mathcal{M}_f^{\mu\nu}. \quad (58)$$

The second amplitude in Fig. 5 is mediated by the triangle loops and is given by the expression

$$\mathcal{M}_f^{\mu\nu}(\chi \rightarrow \gamma\gamma) = \sum_f N_c(f) i C_0(m_\chi^2, m_f) c_{\gamma\gamma}^{\chi,f} \varepsilon[\mu, \nu, k_1, k_2], \quad (59)$$

$$f = \{q_u, q_d, \nu_l, l, \chi_1^\pm, \chi_2^\pm\},$$

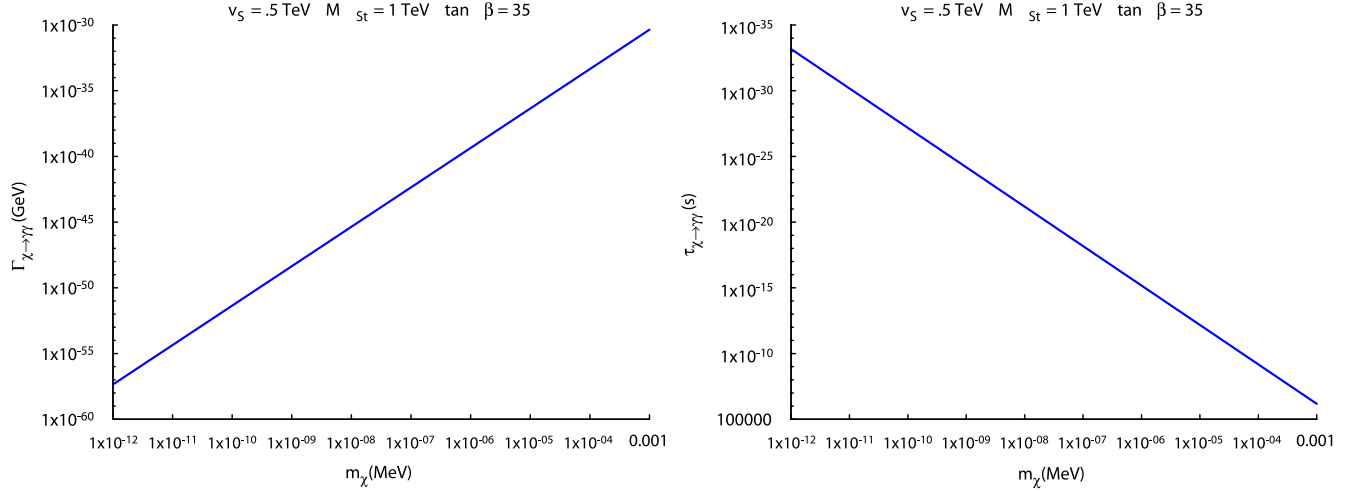
where $N_c(f)$ is the color factor for the fermions. In the domain $0 < m_\chi < 2m_f$, which is the relevant domain for our study, with the axion being very light, the pseudoscalar triangle when both photons are on mass shell is given by the expression

$$C_0(m_\chi^2, m_f) = -\frac{m_f}{\pi^2 m_\chi^2} \arctan^2\left(\left(\frac{4m_f^2}{m_\chi^2} - 1\right)^{-1/2}\right) = -\frac{m_f}{\pi^2 m_\chi^2} \eta(\tau). \quad (60)$$

The coefficient $c_{\gamma\gamma}^{\chi,f}$ is the factor for the vertex between the axi-Higgs and the fermion current. The expressions of these factors are

$$c^{\chi, q_u} = -\frac{i\sqrt{2}y_u M_{\text{St}} v_1^2 v_2}{\sqrt{(v^2 v_S^2 + v_1^2 v_2^2)[4M_{\text{St}}^2 v^2 + g_B B_S (v^2 v_S^2 + v_1^2 v_2^2)]}},$$

$$c^{\chi, q_d} = -\frac{v_2 y_d}{v_1 y_u} c^{\chi, q_u}, \quad c^{\chi, l} = \frac{y_e}{y_d} c^{\chi, q_d}. \quad (61)$$


 FIG. 6 (color online). Decay amplitude (left panel) and mean lifetime (right panel) for $\chi \rightarrow \gamma\gamma$ as a function of the axi-Higgs mass.

We obtain the following expression for the decay amplitude:

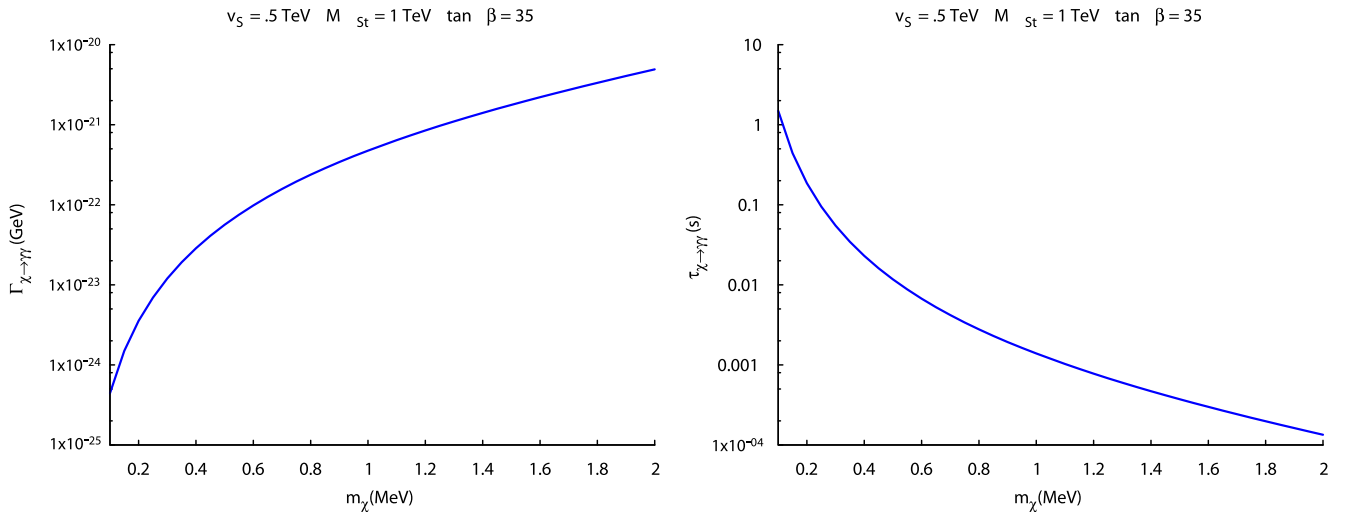
$$\begin{aligned} \Gamma_\chi &\equiv \Gamma(\chi \rightarrow \gamma\gamma) \\ &= \frac{m_\chi^3}{32\pi} \left\{ 8(g_{\gamma\gamma}^\chi)^2 + \frac{1}{2} \left| \sum_f N_c(f) i \frac{\tau_f \eta(\tau_f)}{4\pi^2 m_f} e^2 Q_f^2 c^{\chi f} \right|^2 \right. \\ &\quad \left. + 4g_{\gamma\gamma}^\chi \sum_f N_c(f) i \frac{\tau_f \eta(\tau_f)}{4\pi^2 m_f} e^2 Q_f^2 c^{\chi f} \right\}, \end{aligned} \quad (62)$$

where the three terms correspond, respectively, to the pointlike WZ term, to the 1-loop contribution, and to their interference.

Notice that in the expression of this decay rate both the direct $[(g_{\gamma\gamma}^\chi)^2]$ and the interference $(\sim g_{\gamma\gamma}^\chi)$ contributions are suppressed as inverse powers of the Stückelberg mass,

here taken to be equal to 1 TeV. We have chosen v as the SM electroweak VEV, and for v_S we have chosen the value of 500 GeV. In order to have an acceptable Higgs spectrum, the Yukawa couplings have been set to give the right fermion masses of the standard model, while for g_B and B_S we have chosen $g_B = 0.1$ and $B_S = 4$.

We show in Figs. 6 and 7 results obtained from the numerical evaluation of the decay amplitude as a function of the mass of the axion m_χ , which clearly indicates that the decay rates are very small for a milli-eV particle, although larger than those of the PQ case [30]. We conclude that a PQ-like axion is indeed long lived also in these models and as such could, in principle, contribute to the relic densities of dark matter. For an axion with a mass in the MeV region, instead, the particle is not stable and as such would decay rather quickly. The decay, in this case, is


 FIG. 7 (color online). Decay amplitude and mean lifetime for $\chi \rightarrow \gamma\gamma$ as a function of the axi-Higgs mass for an axion whose mass is in the MeV range.

fast enough ($\tau \lesssim 10^{-3}$ s) and does not interfere with the nucleosynthesis.

VII. COLD DARK MATTER BY MISALIGNMENT OF THE AXION FIELD

In the case of a long-lived axion, the generation of relic densities of axion dark matter, in this model, involves two (sequential) misalignments, generated, as we have already discussed, the first at the electroweak scale, and the second at the QCD phase transition. The presence of two misalignments at two separate scales, as discussed in [30], is typical of axions which show interactions both with the weak and with the strong sectors, due to the presence of mixed anomalies. This point has been addressed in detail within a nonsupersymmetric model, but in a supersymmetric scenario the physical picture remains the same.

In the PQ-like case, at the first misalignment, taking place at the electroweak scale, the physical axion is singled out as a component of $\text{Im}b$, with a mass which is practically zero, due to the small value of the curvature induced by the potential generated by electroweak instantons (Fig. 3, top panel) given in Eq. (40). In the case of a very small extra potential ($\lambda_{\text{eff}} \sim \lambda_{\text{inst}}$) it is the second misalignment that is responsible for generating an axion mass. At the second misalignment, taking place at the QCD phase transition, the mass of this pseudo Nambu-Goldstone mode is redefined from zero to a small but more significant value ($\sim 10^{-3}$ eV) induced by the QCD instantons (Fig. 3, bottom). The final value of the mass is determined in terms of the hadronic scale Λ_{QCD} and of a second intermediate scale, M_{St}^2/v , which replaces f_a in all of the expressions usually quoted in the literature and held valid for PQ axions, as we are now going to clarify.

- (i) *MeV axion*.—An MeV axion is allowed only if the extra potential (the misalignment) is assumed to be generated at a scale different from the electroweak phase transition, say at an earlier time. This misalignment, in fact, should be unrelated to the (quasi-periodic) corrections induced at the electroweak time, as shown in Fig. 4, the latter being of very small size. However, such an axion would not be long lived. One can easily realize that in this scenario, due to the sizable value of m_χ , there is an overlap between the period of coherent oscillations at the QCD hadron transition and the typical lifetime at which the axion decays. This can be trivially checked by comparing the QCD time, defined as the inverse Hubble rate at the temperature of confinement [$H(T_{\text{QCD}}) \sim 10^{-11}$ eV, $T_{\text{QCD}} \sim 200$ MeV] $t_{\text{QCD}} \sim 10^{-4}$ s with the axion lifetime in this typical mass range.
- (ii) *PQ-like axion*.—For a PQ-like axion the effective scale (M_{St}^2/v) is the result of the product of two factors: the first factor due to the rotation matrix of the Stückelberg field $\text{Im}b$ onto χ —which is propor-

tional to v/M —times the second factor ($1/M_{\text{St}}$) which is inherited from the original $\text{Im}b/M_{\text{St}}F\tilde{F}$ (WZ) counterterm. Specifically, starting from Eq. (39), the size of the projection of $\text{Im}b$ into χ is given by

$$\frac{1}{N_\chi} B_S g_B (v^2 v_S^2 + v_1^2 v_2^2) \sim v/M_{\text{St}}, \quad (63)$$

and hence a typical PQ interaction term involving the Stückelberg field b becomes

$$\frac{\text{Im}b}{M_{\text{St}}} FF' \rightarrow \frac{\chi}{M_{\text{St}}^2/v} FF'. \quad (64)$$

The physical state with a b component (i.e. χ) acquires an interaction to $F\tilde{F}$ which is suppressed by the scale M_{St}^2/v .

Having identified this scale, if we neglect the axion mass generated by V' [Eq. (40)] at the electroweak scale, the final mass of the physical axion induced at the QCD scale is controlled by the ratio $m_\chi \sim \Lambda_{\text{QCD}}^2 v/M_{\text{St}}^2$, where the angle of misalignment is given by $\theta' = \chi v/M_{\text{St}}^2$.

Coming to the value of the abundances for a PQ-like axion—defined as the number density to entropy ratio $Y = n_\chi/s$ —these can be computed in terms of the relevant suppression scale appearing in the $\chi F\tilde{F}$ interaction. We have expanded on the structure of the computation in Appendix C. If we indicate with $\theta'(T_i)$ the angle of misalignment at the QCD hadron transition and with T_i the initial temperature at the beginning of the oscillations, the expression of the abundances takes the form

$$Y_\chi(T_i) = \left(\frac{v}{M_{\text{St}}}\right) \frac{45 M_{\text{St}}^2 (\theta'(T_i))^2}{2\sqrt{5}\pi g_{*,T} T_i M_P}, \quad (65)$$

which depends linearly on M_{St} . As we have already mentioned, the computation of the relic densities for a non-thermal population follows rather closely the approach outlined in the nonsupersymmetric case. For instance, a rather large value of M_{St} , of the order of 10^7 GeV [30], determines a sizable contribution of the gauged axion to the relic densities of cold dark matter. These, in turn, follow rather closely the behavior expected in the case of the PQ axion. In practice, to obtain a sizable nonthermal population of gauged axions, M_{St} should be such that $M_{\text{St}}^2/v \sim f_a$, with f_a the usual estimated size of the PQ axion decay constant. This allows a sizable contribution of χ to the relic density of cold dark matter, with a partial contribution to Ω ($\Omega_\chi h^2 \sim 0.1$) in close analogy to what was expected in the case of the PQ axion. These considerations, which are in close relation with what was found in the nonsupersymmetric construction [30], in this case will be subject to the constraints coming from the neutralino sector and its abundances derived from WMAP. We will come back to this point after presenting the results of our simulations in the next sections.

VIII. THE NEUTRALINO SECTOR

The neutralino sector is constructed from the eigenstates of the space spanned by the neutral fields ($i\lambda_{W_3}$, $i\lambda_Y$, $i\lambda_B$, \tilde{H}_1^1 , \tilde{H}_2^2 , \tilde{S} , and $\psi_{\mathbf{b}}$), which involve the three neutral gauginos, the two Higgsinos, the singlino (the fermion component of the singlet superfield), and the axino component of the Stückelberg supermultiplet. We denote with M_{χ_0} the corresponding mass matrix and we list its components in Appendix B. The neutralino eigenstates of this mass matrix are labeled as $\tilde{\chi}_i^0$ ($i = 0, \dots, 6$) and can be expressed in the basis $\{i\lambda_{W_3}, i\lambda_Y, i\lambda_B, \tilde{H}_1^1, \tilde{H}_2^2, \tilde{S}, \psi_{\mathbf{b}}\}$

$$\begin{aligned} \tilde{\chi}_i^0 = & a_{i1}i\lambda_{W_3} + a_{i2}i\lambda_Y + a_{i3}i\lambda_B + a_{i4}\tilde{H}_1^1 + a_{i5}\tilde{H}_2^2 \\ & + a_{i6}\tilde{S} + a_{i7}\psi_{\mathbf{b}}. \end{aligned} \quad (66)$$

The neutralino mass eigenstates are ordered in mass and the lightest eigenstate corresponds to $i = 0$. We indicate with O^{χ^0} the rotation matrix that diagonalizes the neutralino mass matrix. In order to perform a numerical analysis of the model we need to fix some of the parameters, first of all requiring consistency of their choice with the masses of the standard-model particles. For this purpose, the Higgs VEVs v_1 and v_2 have been constrained in order to generate the correct mass values of the W^\pm , which depends on $v^2 = v_1^2 + v_2^2$, and of the Z gauge boson.

The Yukawa couplings have been fixed in order to give the correct masses of the SM fermions. The choice of v_S and of the parameter λ in the trilinear term $\lambda SH_1 \cdot H_2$ in the scalar potential has been made in order to obtain mass values in the Higgs sector in agreement with the limits from direct searches [with $\lambda \sim \mathcal{O}(1)$]. For this reason we have selected the value $\lambda = 0.5$ and the assignment $B_{H_1} = -1$, $B_S = 3$ for the $U(1)_B$ charges of the Higgs and the singlet; $B_Q = 2$ for the quark doublet, and $B_L = 1$ for the lepton doublet. The gauge mass term parameters have been selected according to the relation

$$M_Y : M_W : M_G = 1 : 2 : 6, \quad (67)$$

coming from the unification condition for the gaugino masses. As a further simplification, the sfermion mass parameters M_L , M_Q , m_R , m_D , and m_U have been set to a unique value M_0 . We have also chosen a common value a_0 for the trilinear couplings a_e , a_d , and a_u . With these choices, besides $\tan\beta$, the only other free parameters left are the Stückelberg mass M_{St} , the gaugino mass term for λ_B , denoted by M_B , and the axino mass term, M_b . Our choices are the following:

$$\begin{aligned} M_Y = 500 \text{ GeV}, \quad M_{YB} = 1 \text{ TeV}, \\ M_W = 1 \text{ TeV}, \quad M_G = 3 \text{ TeV}, \\ M_L = M_Q = m_R = m_D = m_U = M_0 = 1 \text{ TeV}, \\ a_e = a_d = a_u = a_0 = 1 \text{ TeV}, \\ a_\lambda = -100 \text{ GeV}, \end{aligned} \quad (68)$$

where with M_L and M_Q we have denoted the scalar mass terms for the sleptons and the squarks, assumed to be equal for all 3 generations. We have also chosen

$$M_B = M_b = 1 \text{ TeV} \quad (69)$$

with a coupling constant g_B of the anomalous $U(1)$ of 0.4. From previous investigations such values of the anomalous coupling are known to be compatible with LEP data at the Z resonance [43,44]. In particular, the mass of the extra Z' ($M_{Z'}$), which in our case is of the order of the Stückelberg mass, $M_{Z'} \sim M_{St}$ [43], due to the region of variability of M_{St} that we investigate in our simulations, obviously satisfies the current LHC constraints at 95% C.L. (> 1140 GeV) from CMS [45] and from ATLAS (> 1.83 TeV) [46] on the absence of a resonance in the dilepton channel at 7 TeV for an extra Z prime with standard-model-like couplings. This parameter choice is our benchmark, which is compatible with all the SM requirements on the spectrum of the known particles. It involves SUSY breaking scales in a kinematical range which is under investigation at the LHC. We also assume a value $v_b = 20$ GeV for the VEV of the saxion field Reb .

The most significant parameters in the relic density calculation are M_{St} and the Higgs VEV ratio $\tan\beta$. Concerning the Stückelberg mass, its value has been chosen to be varied in two different regions, 2–10 TeV and 11–25 TeV. In both regions we will consider different values of $\tan\beta$.

IX. NEUTRALINO RELIC DENSITIES AND COSMOLOGICAL BOUNDS

As is well known, the evaluation of the relic densities requires the calculation of a great number of thermally averaged cross sections, given the number of particles which are present. Before coming to the discussion of the results of this very involved analysis, which is summarized in some simple plots of the relic densities of the lightest neutralino—as a function both of M_{St} and $\tan\beta$ —we present a general description of the structure of the interactions in the model. We also list the 2-to-2 processes that have been considered in the coupled Boltzmann equations.

We start from the action involving the physical axion (H_0^5) and its interactions with the various sectors. These involve, typically, interactions with the Higgs sector via bilinear vertices (proportional to $R^{H_0^5 HH}$), and trilinear ones (proportional to $R^{H_0^5 HHH}$) in H , with H denoting generically CP -even and CP -odd Higgs eigenstates. Other interactions in the same component of the Lagrangian involve axion-neutralino terms ($R^{H_0^5 \chi_i^0 \chi_j^0}$) plus axion charginos ($R^{H_0^5 \chi_i^\pm \chi_j^\mp}$). Other terms are those involving interactions of the axion with the sleptons ($R^{H_0^5 \tilde{l}_i^\dagger \tilde{l}_j}$) and the squarks ($R^{H_0^5 \tilde{q}_i^\dagger \tilde{q}_j}$); vertices involving gauge bosons (for instance $R^{H_0^5 A \chi_i^\pm \chi_j^\mp}$, with a photon A and two charginos) and quartic contributions with 2, 3, and 4 axion lines. The Lagrangian

describing all the tree-level interactions involving the axion is

$$\begin{aligned}
 \mathcal{L}_{H_0^5\text{-int}} = & R^{H_0^5 H_0^4 H_0^5} H_0^5 H_0^4 H_0^5 + R^{H_0^5 H_0^5 (H_0^5)^2} H_0^5 + R^{H_0^5 H_0^4 H_0^5 H_0^4} H_0^5 H_0^4 H_0^5 H_0^4 + R^{H_0^5 H_0^5 (H_0^5)^2} H_0^5 H_0^5 + R^{H_0^5 H_0^4 H_0^5} H_0^5 H_0^4 H_0^5 \\
 & + R^{H_0^5 H_0^4 H_0^5} (H_0^5)^2 (H_0^4)^2 + R^{H_0^5 H_0^4 (H_0^5)^3} H_0^4 + R^{H_0^5 H_0^4 (H_0^5)^4} + R^{H_0^5 \chi_i^0 \chi_j^0} H_0^5 \chi_i^0 \chi_j^0 + R^{H_0^5 \chi_i^\pm \chi_j^\mp} H_0^5 \chi_i^\pm \chi_j^\mp + R^{H_0^5 \tilde{l}_i} H_0^5 \tilde{l}_i^\dagger \tilde{l}_j \\
 & + R^{H_0^5 \tilde{q}_i \tilde{q}_j} H_0^5 \tilde{q}_i^\dagger \tilde{q}_j + R^{H_0^5 A \chi_i^\pm \chi_j^\mp} H_0^5 A \mu \bar{\chi}_i^\pm \gamma_\mu \chi_j^\mp + R^{H_0^5 Z \chi_i^\pm \chi_j^\mp} H_0^5 Z^\mu \bar{\chi}_i^\pm \gamma_\mu \chi_j^\mp + R^{H_0^5 Z' \chi_i^\pm \chi_j^\mp} H_0^5 Z'^\mu \bar{\chi}_i^\pm \gamma_\mu \chi_j^\mp \\
 & + R^{H_0^5 W^\mp \chi_i^\pm \chi_j^0} H_0^5 W_\mu^\mp \bar{\chi}_i^\pm \gamma^\mu \chi_j^0 + R^{\chi_i^0 \chi_j^\pm H^\mp H_0^5} \chi_i^0 \chi_j^\pm H^\mp H_0^5 + R^{\chi_i^0 \chi_j^0 H_0^5 H_0^4} \chi_i^0 \chi_j^0 H_0^5 H_0^4.
 \end{aligned} \tag{70}$$

The explicit expressions of these vertices are rather involved and we omit them. Other interactions appearing in the interaction Lagrangian involve derivative couplings with the gauge bosons and the Higgses and they are given by

$$\mathcal{L}_{H_0^5\text{-int}} = R^{H_0^5 H^\pm W^\mp} H_0^5 W_\mu^\mp \partial^\mu H^\pm + R^{H_0^5 H_0^A} H_0^5 A_\mu \partial^\mu H_0^i + R^{H_0^5 H_0^Z} H_0^5 Z_\mu \partial^\mu H_0^i + R^{H_0^5 H_0^Z'} H_0^5 Z'_\mu \partial^\mu H_0^i. \tag{71}$$

Similar interactions are also typical for H_0^4 , the CP -odd Higgs. Some of the vertices are illustrated in Fig. 8. Besides the interaction with the axi-Higgs, we have the following vertices involving neutralinos:

$$\begin{aligned}
 \mathcal{L}_{\chi_0\text{-int}} = & R^{\chi_i^0 \chi_j^0 Z} Z^\mu \bar{\chi}_i^0 \gamma_\mu \chi_j^0 + R^{\chi_i^0 \chi_j^0 Z'} Z'^\mu \bar{\chi}_i^0 \gamma_\mu \chi_j^0 + R^{\chi_i^0 \chi_j^\pm W^\mp} W_\mu^\mp \bar{\chi}_i^0 \gamma_\mu \chi_j^\pm + R^{\chi_i^0 \chi_j^\pm H^\mp} H^\mp \bar{\chi}_i^0 \gamma_\mu \chi_j^\pm + R^{\chi_i^0 \chi_j^0 H_0^k} H_0^k \bar{\chi}_i^0 \gamma_\mu \chi_j^0 \\
 & + R^{\chi_i^0 f \tilde{f}} \chi_i^0 f \tilde{f}_{1,2} + R^{\chi_i^0 \chi_j^\pm \tilde{q}^\dagger \tilde{q}} \chi_i^0 \chi_j^\pm \tilde{q}_k^\dagger \tilde{q}_l + R^{\chi_i^0 \chi_j^0 \tilde{f}^\dagger \tilde{f}} \chi_i^0 \chi_j^0 \tilde{f}_k^\dagger \tilde{f}_l + R^{\chi_i^0 \chi_j^\pm H^\mp H_0^k} \chi_i^0 \chi_j^\pm H^\mp H_0^k \\
 & + R^{\chi_i^0 \chi_j^0 H_0^k H_0^l} \chi_i^0 \chi_j^0 H_0^k H_0^l + R^{\chi_i^0 \chi_j^0 H^\pm H^\mp} \chi_i^0 \chi_j^0 H^\pm H^\mp.
 \end{aligned} \tag{72}$$

Some of these vertices are illustrated in Fig. 9. The full Lagrangian has been implemented using the FEYNRULES [47] package. The same package allows one to generate the CALCHEP [48] model files which are needed by MICROMEAS [49] for the calculation of the scattering cross section that are required in the relic density calculation.

With our choice for the parameters the lightest neutralino is the lightest supersymmetric particle and so it is the dark matter component in our simulations. The value of the neutralino mass in this case turns out to be around 23 GeV with a rather mild dependence on $\tan\beta$. For $\tan\beta$ varying

between 5 and 25 the neutralino mass varies from 22.4 to 23.8 GeV.

We show in Table I a list of the most relevant 2-to-2 processes which are generated in the s , t , and u channels having neutralinos in the initial state (in), while the possible final states are shown on the right-hand side of the same table (out).

In Fig. 10 we show the results obtained for the lightest neutralino relic density with M_{St} in the range 5–8 TeV, $v_S = 600$ GeV, and a varying $\tan\beta$. The values of v_S , $\tan\beta$, and M_{St} for which we plot the result coming from

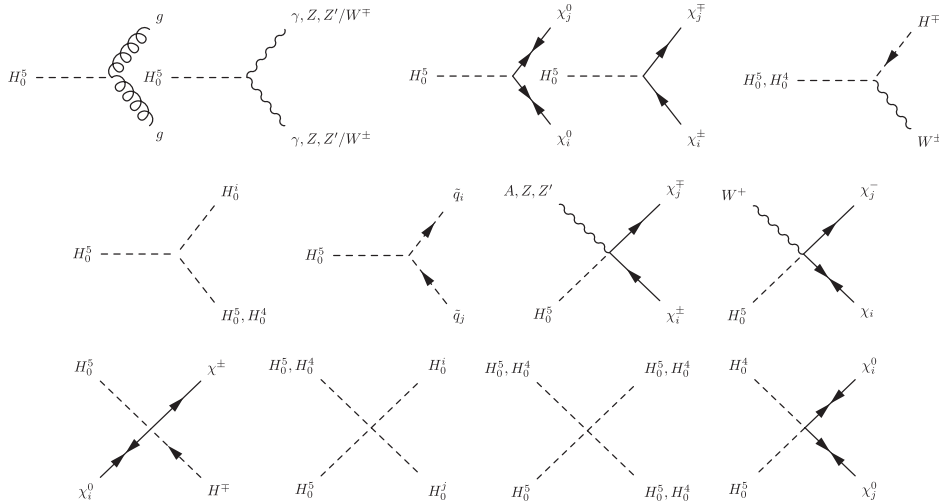


FIG. 8. Axi-Higgs (H_0^5) interactions. The double arrows denote Majorana particles (neutralinos).

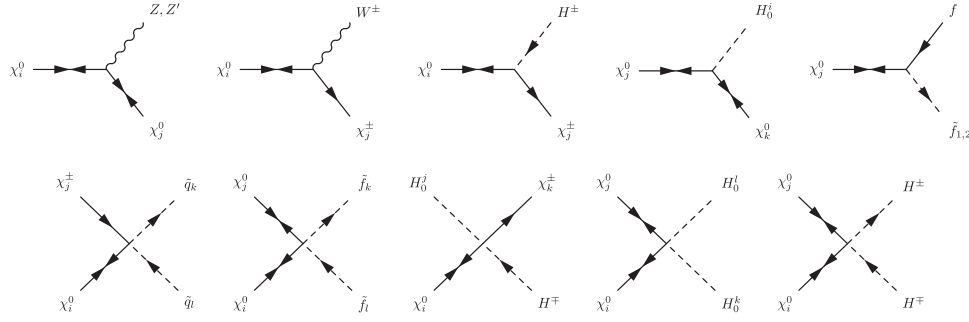


FIG. 9. Neutralino interactions.

the relic density calculation are those that give also acceptable mass values for the whole spectrum, in particular, for the neutral Higgs ($\sim 124\text{--}126$ GeV) [50,51]. The horizontal bar represents the experimental value for the physical dark matter density measured by WMAP, $\Omega h^2 = 0.1123 \pm 0.0035$ [52]. In Fig. 11 we show the analogous results obtained in the range 11–24 TeV with $v_S = 1.2$ TeV and varying $\tan\beta$. Once again these values are such that we obtain acceptable values for the masses of all the particles in the model. One can immediately notice that for a fixed value of $\tan\beta$ as we increase M_{St} , the relic densities grow and tend to violate the WMAP bound. This trend has been found over a sizable range of variability of $\tan\beta$ and is a central feature of the model. It is then obvious, from the same figures, that it is possible to raise the Stückelberg mass and stay below the bound if, at the same time, we increase $\tan\beta$.

X. SUMMARY: WINDOWS ON THE AXION MASS

At this point, before coming to our conclusions, we can try to gather all the information that we have obtained so far in the previous sections, summarizing the basic properties of axions in these types of models.

- (i) *The milli-eV (PQ-like) axion.*—One possibility that we have explored in this work is that V' , the extra potential which is periodic in the axion field, may be generated around the TeV scale or at the electroweak phase transition. The actual strength of the potential remains, in our construction, undetermined and the physical features of the axion (primarily its mass)

depend on this parameter. We have tried to describe the various possibilities, in this respect, and the essential features for each choice for the value of the mass. In particular, if the extra potential is generated by nonperturbative effects at the electroweak phase transition, then the mass of the axion is tiny and the true mechanism of misalignment which determines its mass takes place at a second stage, at the QCD phase transition. In this case the physical axion of the model would not be much different from an ordinary PQ axion and would be rather long lived. At the same time, its abundances are fixed by the possible value of the scale M_{St}^2/v , which should be rather large ($\sim 10^{10}\text{--}10^{12}$ GeV), of the same order of f_a in typical axion models, to be a significant component of cold dark matter. In the region that we have analyzed numerically, with M_{St} around the 2–20 TeVs, the contribution to dark matter from misalignment of the axion field, in this case, should be small.

A second important constraint on this particle, in this mass range, comes from direct axion searches, which also requires the interaction of the axions with the gauge fields (in particular the photon) to be suppressed by a large f_a . For this reason, with M_{St} in the TeV region, these simulations indicate that an axion of this mass, in fact, can be excluded by typical searches with detectors of the Sikivie type. The reason is rather obvious, since axions in the milli-eV mass range could be copiously produced at the center of the Sun and probably should have

TABLE I. Tree-level neutralino annihilation processes in the 3 kinematic channels.

In	s channel	Out
$\chi_i^0 \chi_j^0$	Z, Z'	$H^\pm H^\mp, H_0^k H_0^4, H_0^k H_0^5, Z/Z' H_0^k, \tilde{f}f, \tilde{f}^\dagger \tilde{f}$
	H_0^k	$H^\pm H^\mp, H_0^l H_0^m, H_0^4 H_0^4, H_0^4 H_0^5, H_0^5 H_0^5, Z/Z' H_0^4/H_0^5, W^\pm H^\mp, Z/Z'/Z/Z', W^\pm W^\mp, \tilde{f}f, \tilde{f}^\dagger \tilde{f}$
	H_0^4, H_0^5	$H_0^k H_0^4, H_0^k H_0^5, Z/Z' H_0^k, W^\pm H^\mp, \tilde{f}f, \tilde{f}^\dagger \tilde{f}$
In	t/u channel	Out
$\chi_i^0 \chi_j^0$	χ_k^0	$H_0^l H_0^m, H_0^l H_0^4/H_0^5, H_0^4/H_0^5 H_0^4/H_0^5, Z/Z' H_0^l/H_0^4/H_0^5, Z/Z'/Z/Z'$
	χ_k^\pm	$W^\pm/H^\pm W^\mp/H^\mp$
	\tilde{f}	$\tilde{f}f$

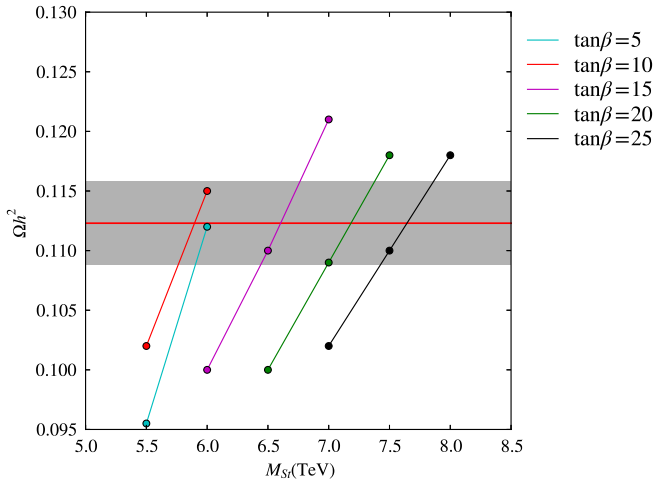


FIG. 10 (color online). Relic density of the lightest neutralino as a function of the Stückelberg mass in the region 5–8.5 TeV for different values of the Higgs VEV ratio $\tan\beta$.

been seen by now in ground based detectors (helioscopes), such as CAST [53]. We recall that one of the goals of searches with helioscopes is to set a lower bound on the suppression scale f_a of the axion-photon vertex, which is currently experimentally constrained, as we have already mentioned, to be rather large.

- (ii) *The meV axion.*—A second possibility that we have investigated is that the extra potential appearing in the CP -odd sector is unrelated to instanton corrections in the electroweak vacuum. In this case the mass of the axion remains a free parameter. The range that we have explored in this second case involves an axion mass in the MeV region, discussing several constraints that emerge from the model.

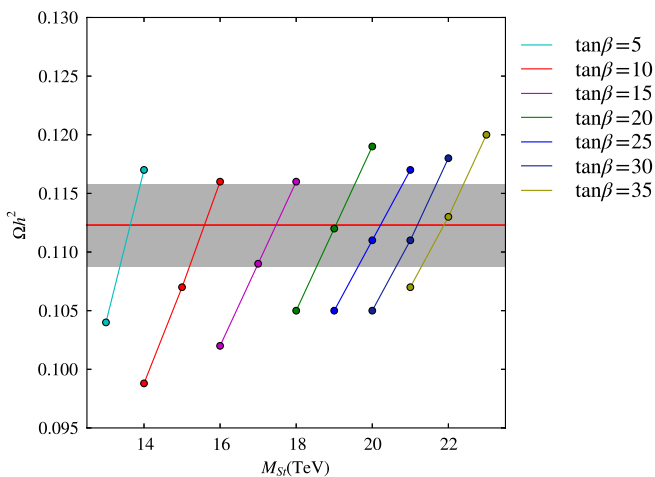


FIG. 11 (color online). Relic density of the lightest neutralino as a function of the Stückelberg mass in the region 2–24 TeV for different values of the Higgs VEV ratio $\tan\beta$.

In this case the axion is, in general, not long lived and as such is not a component of dark matter. On the other hand, the constraints from CAST can be avoided, since the particle would not be produced by ordinary thermal mechanisms at the center of the Sun, where the temperature is about 1.7 keV, being its mass above the keV range. Obviously, in this case other constraints emerge from nucleosynthesis requirements, since a particle in this mass range has to decay fast enough in order not to generate a late entropy release at nucleosynthesis time. We have seen that an axion in the MeV range is consistent with these two requirements. An axion of this type could be searched for at colliders, and in this respect the analysis of its possible detection at the LHC would follow quite closely the patterns described by two of us in [41]. As in this previous (nonsupersymmetric) study, where the axion is Higgs like (of a mass in the GeV region), typical channels of where to look for this particle would be (a) the associated production of an axion and a direct photon, (b) the multi-axion production channel, and (c) the associated production of one axion and other Higgses of the CP -even sector. The modifications, compared to that previous study, would now involve (1) the lower value of the mass of the axion (MeV rather than GeV), and (2) the presence of extra supersymmetric interactions.

Comments.—One important comment concerns the connection between these classes of models and their completion theories such as string theory, which lay at their foundation. In our study we have selected a scenario characterized by low energy supersymmetry, with a phenomenological analysis that is essentially connected with the TeV scale and above. This is the scale which is likely to be scanned in the near future by several experiments, including the LHC, and for this reason we have directed our numerical studies in this direction. There is, however, a second case that involves a value of M_{St} which is very large and close to the Planck scale. In this second case the model predicts, obviously, a decoupling of the anomalous symmetry, leaving at low energy a scenario which is essentially the same as that of the MSSM, since the extra Z prime, which is part of the spectrum, is extremely heavy. This would obviously imply a decoupling both of the anomalous gauge boson and of the anomalous trilinear interactions which are associated with it. A physical axion could, however, survive this limit, if the scale of the extra potential is also of the order of M_{St} , but its interaction with ordinary matter would be extremely suppressed by the same scale.

XI. CONCLUSIONS

We believe the investigation of the phenomenological role played by models containing anomalous gauge

interactions from Abelian extensions of the standard model will receive further attention in the future. These studies can be motivated within several scenarios, including string and supergravity theories, in which gauged axionic symmetries are introduced for anomaly cancellation. In turn, these modified mechanisms of cancellation of the anomalies, which involve an anomalous fermion spectrum and an axion, are essentially connected with the UV completion of these field theories, which in a string framework is realized by the Green-Schwarz mechanism.

The model that we have investigated (the USSM-A) summarizes the most salient physical features of these types of constructions, where a Stückelberg supermultiplet is associated with an anomalous Abelian structure in order to restore the gauge invariance of the anomalous effective action. In this work we have tried to characterize in detail some of the main phenomenological implications of these models, which are particularly interesting for cosmology. The physical axion of this construction, or gauged axion, emerges as a component of the Stückelberg field $\text{Im}b$. We have pointed out that the mechanism of sequential misalignment, formerly discussed in the nonsupersymmetric case [30], finds a natural application also in the presence of supersymmetry, with minor modifications.

One relevant feature of these models, already noticed in [30], is that their axions do not contribute to the isocurvature perturbations of the early universe, being gauge degrees of freedom at the scale of inflation.

We have followed a specific pattern in order to come out with specific results in these types of models, using for this purpose a particular superpotential (the USSM superpotential), whose essential features, however, may well be generic.

We have presented an accurate study of the neutralino relic densities, showing that the Stückelberg mass value is constrained by the requirement of a consistent mass spectrum, with values for the lightest CP -even Higgs larger than the current LHC limits (>120 GeV) and by the experimental value for the dark matter abundance from WMAP [52]. Thus, in these models, the allowed value of the Stückelberg scale is positively correlated with the value of $\tan\beta$. As it grows, $\tan\beta$ has also to grow (for a fixed value of the VEV of the singlet ν_S) in order to preserve the WMAP bound. In particular M_{St} and ν_S are positively correlated. This correlation is necessary in order to obtain values of the neutralino mass which allow one to satisfy the same bounds, which in our case is around 20 GeV.

We have seen that with a Stückelberg mass in the TeV range the nonthermal population of axions does not contribute significantly to the dark matter densities if these axions are PQ like. These types of constraints, obviously, are typical of supersymmetric constructions and are avoided in a nonsupersymmetric context. In this second

case, as discussed in [30], a Stückelberg scale around 10^7 GeV is sufficient to revert this trend.

We have also pointed out that gauged axions in the milli-eV mass range are probably difficult to reconcile with current bounds from direct searches, while the case for detecting MeV or heavier axions, in these types of models, remains a wide open possibility. In this second case, cascade decays of these light particles and their associated production with photons should be seen as their possible event signatures at the LHC.

ACKNOWLEDGMENTS

We thank Nikos Irges, George Lazarides, and Antonio Racioppi for discussions. This work is supported in part by the European Union through the Marie Curie Research and Training Network UniverseNet (No. MRTN-CT-2006-035863).

APPENDIX A: GENERAL FEATURES OF THE MODEL

In this Appendix we summarize some of the basic features of the USSM-A. The gauge structure of the model is of the form $\text{SU}(3)_c \times \text{SU}(2) \times \text{U}(1)_Y \times \text{U}(1)_B$, where B is the anomalous gauge boson, and with a matter content given by the usual generations of the SM. In all the Lagrangians below we implicitly sum over the three fermion generations. A list of the fundamental superfields and charge assignments is summarized in Table II. The Lagrangian can be expressed as

$$\mathcal{L}_{\text{USSM-A}} = \mathcal{L}_{\text{USSM}} + \mathcal{L}_{\text{KM}} + \mathcal{L}_{\text{FI}} + \mathcal{L}_{\text{axion}}, \quad (\text{A1})$$

where the Lagrangian of the USSM ($\mathcal{L}_{\text{USSM}}$) has been modified by the addition of $\mathcal{L}_{\text{axion}}$ to compensate for the anomalous variation of the corresponding effective action due to the anomalous charge assignments. The former is given by

$$\begin{aligned} \mathcal{L}_{\text{USSM}} = & \mathcal{L}_{\text{lep}} + \mathcal{L}_{\text{quark}} + \mathcal{L}_{\text{Higgs}} + \mathcal{L}_{\text{gauge}} \\ & + \mathcal{L}_{\text{SMT}} + \mathcal{L}_{\text{GMT}} \end{aligned} \quad (\text{A2})$$

TABLE II. Charge assignment of the model.

Superfields	SU(3)	SU(2)	U(1) _Y	U(1) _B
$\hat{\mathbf{b}}(x, \theta, \bar{\theta})$	1	1	0	s
$\hat{S}(x, \theta, \bar{\theta})$	1	1	0	B_S
$\hat{L}(x, \theta, \bar{\theta})$	1	2	-1/2	B_L
$\hat{R}(x, \theta, \bar{\theta})$	1	1	1	B_R
$\hat{Q}(x, \theta, \bar{\theta})$	3	2	1/6	B_Q
$\hat{U}_R(x, \theta, \bar{\theta})$	$\bar{\mathbf{3}}$	1	-2/3	B_{U_R}
$\hat{D}_R(x, \theta, \bar{\theta})$	$\bar{\mathbf{3}}$	1	+1/3	B_{D_R}
$\hat{H}_1(x, \theta, \bar{\theta})$	1	2	-1/2	B_{H_1}
$\hat{H}_2(x, \theta, \bar{\theta})$	1	2	1/2	B_{H_2}

with contributions from the leptons, quarks, and Higgs plus gauge kinetic terms. The matter contributions from leptons and quarks

$$\mathcal{L}_{\text{lep}} = \int d^4\theta [\hat{L}^\dagger e^{2g_2\hat{W}+g_Y\hat{Y}+g_B\hat{B}} \hat{L} + \hat{R}^\dagger e^{2g_2\hat{W}+g_Y\hat{Y}+g_B\hat{B}} \hat{R}], \quad (\text{A3})$$

$$\mathcal{L}_{\text{quark}} = \int d^4\theta [\hat{Q}^\dagger e^{2g_s\hat{G}+2g_2\hat{W}+g_Y\hat{Y}+g_B\hat{B}} \hat{Q} + \hat{U}_R^\dagger e^{2g_s\hat{G}+g_Y\hat{Y}+g_B\hat{B}} \hat{U}_R + \hat{D}_R^\dagger e^{2g_s\hat{G}+g_Y\hat{Y}+g_B\hat{B}} \hat{D}_R] \quad (\text{A4})$$

are accompanied by a sector which involves two Higgs SU(2) doublet superfields, \hat{H}_1 and \hat{H}_2 , and one singlet \hat{S}

$$\mathcal{L}_{\text{gauge}} = \frac{1}{4} \int d^4\theta [\mathcal{G}^\alpha \mathcal{G}_\alpha + W^\alpha W_\alpha + W^{Y\alpha} W_\alpha^Y + W^{B\alpha} W_\alpha^B] \delta^2(\bar{\theta}) + \text{H.c.},$$

$$\mathcal{L}_{\text{SMT}} = - \int d^4\theta \delta^4(\theta, \bar{\theta}) [M_L^2 \hat{L}^\dagger \hat{L} + m_R^2 \hat{R}^\dagger \hat{R} + M_Q^2 \hat{Q}^\dagger \hat{Q} + m_U^2 \hat{U}_R^\dagger \hat{U}_R + m_D^2 \hat{D}_R^\dagger \hat{D}_R + m_1^2 \hat{H}_1^\dagger \hat{H}_1 + m_2^2 \hat{H}_2^\dagger \hat{H}_2 + m_S^2 \hat{S}^\dagger \hat{S} + (a_\lambda \hat{S} \hat{H}_1 \cdot \hat{H}_2 + \text{H.c.}) + (a_e \hat{H}_1 \cdot \hat{L} \hat{R} + \text{H.c.}) + (a_d \hat{H}_1 \cdot \hat{Q} \hat{D}_R + \text{H.c.}) + (a_u \hat{H}_2 \cdot \hat{Q} \hat{U}_R + \text{H.c.})]. \quad (\text{A7})$$

As usual, $M_L, M_Q, m_R, m_{U_R}, m_{D_R}, m_1, m_2$, and m_S are the mass parameters of the explicit supersymmetry breaking, while a_e, a_λ, a_u , and a_d are dimensionful coefficients. The soft breaking due to gaugino mass terms (GMT) now includes a mixing mass parameter M_{YB}

$$\mathcal{L}_{\text{GMT}} = \int d^4\theta \left[\frac{1}{2} (M_G \mathcal{G}^\alpha \mathcal{G}_\alpha + M_w W^\alpha W_\alpha + M_Y W^{Y\alpha} W_\alpha^Y + M_B W^{B\alpha} W_\alpha^B + M_{YB} W^{Y\alpha} W_\alpha^B) + \text{H.c.} \right] \delta^4(\theta, \bar{\theta}). \quad (\text{A8})$$

The superfield $\hat{\mathbf{b}}$ describes the Stückelberg multiplet,

$$\hat{\mathbf{b}} = b + \sqrt{2}\theta\psi_{\mathbf{b}} - i\theta\sigma^\mu\bar{\theta}\partial_\mu b + \frac{i}{\sqrt{2}}\theta\theta\bar{\theta}\bar{\sigma}^\mu\partial_\mu\psi_{\mathbf{b}} - \frac{1}{4}\theta\theta\bar{\theta}\bar{\theta}\square b - \theta\theta F_{\mathbf{b}}, \quad (\text{A9})$$

and contains the Stückelberg axion (a complex b field) and its supersymmetric partner, referred to as the axino ($\psi_{\mathbf{b}}$), which combines with the neutral gauginos and Higgsinos to generate the neutralinos of the model. Details on the notation for the superfields components can be found in Table III. We recall that we denote with λ_B and λ_Y the two gauginos of the two vector superfields (\hat{B}, \hat{Y}) corresponding to the anomalous U(1)_B and to the hypercharge vector multiplet. The singlet superfield \hat{S} has as components the scalar ‘‘singlet’’ S and its supersymmetric partner, the singlino, denoted as \tilde{S} .

$$\mathcal{L}_{\text{Higgs}} = \int d^4\theta [\hat{H}_1^\dagger e^{2g_2\hat{W}+g_Y\hat{Y}+g_B\hat{B}} \hat{H}_1 + \hat{H}_2^\dagger e^{2g_2\hat{W}+g_Y\hat{Y}+g_B\hat{B}} \hat{H}_2 + \hat{S}^\dagger e^{g_B\hat{B}} \hat{S} + \mathcal{W} \delta^2(\bar{\theta}) + \bar{\mathcal{W}} \delta^2(\theta)] \quad (\text{A5})$$

with the superpotential chosen of the form

$$\mathcal{W} = \lambda \hat{S} \hat{H}_1 \cdot \hat{H}_2 + y_e \hat{H}_1 \cdot \hat{L} \hat{R} + y_d \hat{H}_1 \cdot \hat{Q} \hat{D}_R + y_u \hat{H}_2 \cdot \hat{Q} \hat{U}_R. \quad (\text{A6})$$

This superpotential, as shown in [34,35], allows a physical axion in the spectrum. The gauge content plus the soft breaking terms in the form of scalar mass terms (SMT) are identical to those of the USSM

The interactions and dynamics of the axion superfield are defined in $\mathcal{L}_{\text{axion}}$, the Lagrangian that contains both the kinetic (Stückelberg) term, responsible for the mass of the anomalous gauge boson (which reaches the electroweak symmetry breaking scale already in a massive state), the kinetic term of the saxion and of the axino, and the Wess-Zumino terms, which are needed for anomaly cancellation. We recall that Stückelberg fields appear both in anomalous and in nonanomalous contexts. The second one has been analyzed recently in [54].

The extra contributions to $\mathcal{L}_{\text{axion}}$, called $\mathcal{L}_{\text{axion},i}$ are given by

TABLE III. Superfields and their components.

Superfield	Bosonic	Fermionic	Auxiliary
$\hat{\mathbf{b}}(x, \theta, \bar{\theta})$	$b(x)$	$\psi_{\mathbf{b}}(x)$	$F_{\mathbf{b}}(x)$
$\hat{S}(x, \theta, \bar{\theta})$	$S(x)$	$\tilde{S}(x)$	$F_S(x)$
$\hat{L}(x, \theta, \bar{\theta})$	$\tilde{L}(x)$	$L(x)$	$F_L(x)$
$\hat{R}(x, \theta, \bar{\theta})$	$\tilde{R}(x)$	$\bar{R}(x)$	$F_R(x)$
$\hat{Q}(x, \theta, \bar{\theta})$	$\tilde{Q}(x)$	$Q(x)$	$F_Q(x)$
$\hat{U}_R(x, \theta, \bar{\theta})$	$\tilde{U}_R(x)$	$\bar{U}_R(x)$	$F_{U_R}(x)$
$\hat{D}_R(x, \theta, \bar{\theta})$	$\tilde{D}_R(x)$	$\bar{D}_R(x)$	$F_{D_R}(x)$
$\hat{H}_1(x, \theta, \bar{\theta})$	$H_1(x)$	$\tilde{H}_1(x)$	$F_{H_1}(x)$
$\hat{H}_2(x, \theta, \bar{\theta})$	$H_2(x)$	$\tilde{H}_2(x)$	$F_{H_2}(x)$
$\hat{B}(x, \theta, \bar{\theta})$	$B_\mu(x)$	$\lambda_B(x)$	$D_B(x)$
$\hat{Y}(x, \theta, \bar{\theta})$	$A_\mu^Y(x)$	$\lambda_Y(x)$	$D_Y(x)$
$\hat{W}^i(x, \theta, \bar{\theta})$	$W_\mu^i(x)$	$\lambda_{W^i}(x)$	$D_{W^i}(x)$
$\hat{G}^a(x, \theta, \bar{\theta})$	$G_\mu^a(x)$	$\lambda_{g^a}(x), \bar{\lambda}_{g^a}(x)$	$D_{G^a}(x)$

$$\begin{aligned}
\mathcal{L}_{\text{axion},i} = & M_{\text{St}} \text{Re} b D_B + M_{\text{St}} (i \psi_{\mathbf{b}} \lambda_B + \text{H.c.}) + \frac{c_G}{M_{\text{St}}} \left(\frac{1}{16} F_{\mathbf{b}} \lambda_G^a \lambda_G^a + \frac{i}{8\sqrt{2}} D_G^a \lambda_G^a \psi_{\mathbf{b}} - \frac{1}{16\sqrt{2}} G_{\mu\nu}^a \psi_{\mathbf{b}} \sigma^\mu \bar{\sigma}^\nu \lambda_G^a \right. \\
& + \frac{1}{64\sqrt{2}} \text{Im} b \tilde{G}^{a\mu\nu} G_{\mu\nu}^a + \frac{1}{8\sqrt{2}} \text{Im} b \lambda_G^a \sigma_\mu D^\mu \bar{\lambda}_G^a + \frac{1}{16\sqrt{2}} \text{Re} b D_G^a D_G^a - \frac{1}{16\sqrt{2}} \text{Re} b G^{a\mu\nu} G_{\mu\nu}^a \\
& \left. - \frac{i}{8\sqrt{2}} \text{Re} b \lambda_G^a \sigma_\mu D^\mu \bar{\lambda}_G^a + \text{H.c.} \right) + \frac{c_W}{M_{\text{St}}} \left(\frac{1}{16} F_{\mathbf{b}} \lambda_W^i \lambda_W^i + \frac{i}{8\sqrt{2}} D_W^i \lambda_W^i \psi_{\mathbf{b}} - \frac{1}{16\sqrt{2}} W_{\mu\nu}^i \psi_{\mathbf{b}} \sigma^\mu \bar{\sigma}^\nu \lambda_W^i \right. \\
& + \frac{1}{64\sqrt{2}} \text{Im} b \tilde{W}^{i\mu\nu} W_{\mu\nu}^i + \frac{1}{8\sqrt{2}} \text{Im} b \lambda_W^i \sigma_\mu D^\mu \bar{\lambda}_W^i + \frac{1}{16\sqrt{2}} \text{Re} b D_W^i D_W^i - \frac{1}{16\sqrt{2}} \text{Re} b W^{i\mu\nu} W_{\mu\nu}^i \\
& \left. - \frac{i}{8\sqrt{2}} \text{Re} b \lambda_W^i \sigma_\mu D^\mu \bar{\lambda}_W^i + \text{H.c.} \right) + \frac{c_Y}{M_{\text{St}}} \left(\frac{1}{2} F_{\mathbf{b}} \lambda_Y \lambda_Y + \frac{i}{\sqrt{2}} D_Y \lambda_Y \psi_{\mathbf{b}} - \frac{1}{2\sqrt{2}} F_{\mu\nu}^Y \psi_{\mathbf{b}} \sigma^\mu \bar{\sigma}^\nu \lambda_Y + \frac{1}{8\sqrt{2}} \text{Im} b \tilde{F}^{Y\mu\nu} F_{\mu\nu}^Y \right. \\
& - \frac{1}{\sqrt{2}} \text{Im} b \lambda_Y \sigma_\mu \partial^\mu \bar{\lambda}_Y + \frac{1}{2\sqrt{2}} \text{Re} b D_Y D_Y - \frac{1}{2\sqrt{2}} \text{Re} b F^{Y\mu\nu} F_{\mu\nu}^Y - \frac{i}{\sqrt{2}} \text{Re} b \lambda_Y \sigma_\mu \partial^\mu \bar{\lambda}_Y + \text{H.c.} \left. \right) + \frac{c_B}{M_{\text{St}}} \left(\frac{1}{2} F_{\mathbf{b}} \lambda_B \lambda_B \right. \\
& + \frac{i}{\sqrt{2}} D_B \lambda_B \psi_{\mathbf{b}} - \frac{1}{2\sqrt{2}} F_{\mu\nu}^B \psi_{\mathbf{b}} \sigma^\mu \bar{\sigma}^\nu \lambda_B + \frac{1}{8\sqrt{2}} \text{Im} b \tilde{F}^{B\mu\nu} F_{\mu\nu}^B - \frac{1}{\sqrt{2}} \text{Im} b \lambda_B \sigma_\mu \partial^\mu \bar{\lambda}_B + \frac{1}{2\sqrt{2}} \text{Re} b D_B D_B \\
& \left. - \frac{1}{2\sqrt{2}} \text{Re} b F^{B\mu\nu} F_{\mu\nu}^B - \frac{i}{\sqrt{2}} \text{Re} b \lambda_B \sigma_\mu \partial^\mu \bar{\lambda}_B + \text{H.c.} \right) + \frac{c_{YB}}{M_{\text{St}}} \left(-\frac{1}{2} F_{\mathbf{b}} \lambda_B \lambda_Y - \frac{i}{2\sqrt{2}} D_Y \lambda_B \psi_{\mathbf{b}} - \frac{i}{2\sqrt{2}} D_B \lambda_Y \psi_{\mathbf{b}} \right. \\
& + \frac{1}{4\sqrt{2}} F_{\mu\nu}^B \psi_{\mathbf{b}} \sigma^\mu \bar{\sigma}^\nu \lambda_Y + \frac{1}{4\sqrt{2}} F_{\mu\nu}^Y \psi_{\mathbf{b}} \sigma^\mu \bar{\sigma}^\nu \lambda_B - \frac{1}{8\sqrt{2}} \text{Im} b \tilde{F}^{Y\mu\nu} F_{\mu\nu}^B + \frac{1}{2\sqrt{2}} \text{Im} b \lambda_Y \sigma_\mu \partial^\mu \bar{\lambda}_B + \frac{1}{2\sqrt{2}} \text{Im} b \lambda_B \sigma_\mu \partial^\mu \bar{\lambda}_Y \\
& \left. - \frac{1}{2\sqrt{2}} \text{Re} b D_Y D_B + \frac{1}{2\sqrt{2}} \text{Re} b F^{Y\mu\nu} F_{\mu\nu}^B - \frac{i}{2\sqrt{2}} \text{Re} b \lambda_Y \sigma_\mu \partial^\mu \bar{\lambda}_B - \frac{i}{2\sqrt{2}} \text{Re} b \lambda_B \sigma_\mu \partial^\mu \bar{\lambda}_Y + \text{H.c.} \right).
\end{aligned} \tag{A10}$$

We finally recall that the three scalar sectors of the model are characterized in terms of

- (i) *A charged Higgs sector.*—This sector involves the states $(\text{Re}H_1^+, \text{Re}H_2^+)$. The mass matrix has one zero eigenvalue corresponding to a charged Goldstone boson and a mass eigenvalue corresponding to the charged Higgs mass

$$m_{H^\pm}^2 = \left(\frac{v_1}{v_2} + \frac{v_2}{v_1} \right) \left(\frac{1}{4} g^2 v_1 v_2 - \frac{1}{2} \lambda^2 v_1 v_2 + a_\lambda \frac{v_S}{\sqrt{2}} \right), \tag{A11}$$

where $g^2 = g_2^2 + g_Y^2$.

- (ii) *A CP-even sector.*—This sector is diagonalized starting from the basis $(\text{Re}H_1^+, \text{Re}H_2^+, \text{Re}S, \text{Re}b)$. The four physical states obtained in this sector are denoted as H_0^1, H_0^2, H_0^3 , and H_0^4 . Together with the charged physical state extracted before, H^\pm , they describe the 6 degrees of freedom of the CP-even sector.

- (iii) *A CP-odd sector.*—This sector is diagonalized starting from the basis $(\text{Im}H_1^+, \text{Im}H_2^+, \text{Im}S, \text{Im}b)$. We obtain two physical states, H_0^5 and H_0^6 , and two Goldstone modes that provide the longitudinal degrees of freedom for the neutral gauge bosons, Z and Z' .

APPENDIX B: NEUTRALINO MASS MATRIX

Now we turn to the neutralino sector; the mass matrix in the basis $(i\lambda_{w_3}, i\lambda_Y, i\lambda_B, \tilde{H}_1^+, \tilde{H}_2^+, \tilde{S}, \psi_{\mathbf{b}})$ takes the form

$$M_{\chi^0} = \begin{pmatrix} M_{\chi^0}^{11} & 0 & 0 & M_{\chi^0}^{14} & M_{\chi^0}^{15} & 0 & M_{\chi^0}^{17} \\ \cdot & M_{\chi^0}^{22} & M_{\chi^0}^{23} & M_{\chi^0}^{24} & M_{\chi^0}^{25} & 0 & 0 \\ \cdot & \cdot & M_{\chi^0}^{33} & M_{\chi^0}^{34} & M_{\chi^0}^{35} & M_{\chi^0}^{36} & M_{\chi^0}^{37} \\ \cdot & \cdot & \cdot & 0 & M_{\chi^0}^{45} & M_{\chi^0}^{46} & 0 \\ \cdot & \cdot & \cdot & \cdot & 0 & M_{\chi^0}^{56} & 0 \\ \cdot & \cdot & \cdot & \cdot & \cdot & 0 & 0 \\ \cdot & \cdot & \cdot & \cdot & \cdot & \cdot & M_{\chi^0}^{77} \end{pmatrix}, \tag{B1}$$

with

$$\begin{aligned}
M_{\chi^0}^{11} &= M_w, & M_{\chi^0}^{14} &= -\frac{g_2 v_1}{2}, & M_{\chi^0}^{15} &= \frac{g_2 v_2}{2}, \\
M_{\chi^0}^{17} &= 0, & M_{\chi^0}^{22} &= M_Y, & M_{\chi^0}^{23} &= \frac{1}{2} M_{YB}, \\
M_{\chi^0}^{24} &= \frac{g_Y v_1}{2}, & M_{\chi^0}^{25} &= -\frac{g_Y v_2}{4}, & M_{\chi^0}^{33} &= \frac{1}{2} M_B, \\
M_{\chi^0}^{34} &= -v_1 g_B B_{H_1}, & M_{\chi^0}^{35} &= -v_2 g_B B_{H_2}, \\
M_{\chi^0}^{36} &= -v_S g_B B_S, & M_{\chi^0}^{37} &= M_{\text{St}}, & M_{\chi^0}^{45} &= \frac{\lambda v_S}{\sqrt{2}}, \\
M_{\chi^0}^{46} &= \frac{\lambda v_2}{\sqrt{2}}, & M_{\chi^0}^{56} &= \frac{\lambda v_1}{\sqrt{2}}, & M_{\chi^0}^{77} &= -M_b.
\end{aligned} \tag{B2}$$

The rotation matrix for this sector is implicitly defined as O^{χ^0} and

$$\begin{pmatrix} i\lambda_{w_3} \\ i\lambda_Y \\ i\lambda_B \\ \tilde{H}_1^1 \\ \tilde{H}_2^2 \\ \tilde{S} \\ \psi_{\mathbf{b}} \end{pmatrix} = O^{\chi^0} \begin{pmatrix} \chi_0^0 \\ \chi_1^0 \\ \chi_2^0 \\ \chi_3^0 \\ \chi_4^0 \\ \chi_5^0 \\ \chi_6^0 \end{pmatrix}. \quad (\text{B3})$$

Chargino sector.—We recall here the structure of the chargino sector and the diagonalization procedure. We define

$$\lambda_{w^+} = \frac{1}{\sqrt{2}}(\lambda_{w_1} - i\lambda_{w_2}), \quad \lambda_{w^-} = \frac{1}{\sqrt{2}}(\lambda_{w_1} + i\lambda_{w_2}), \quad (\text{B4})$$

and in the basis $(\lambda_{w^+}, \tilde{H}_2^1, \lambda_{w^-}, \tilde{H}_1^2)$ we obtain the mass matrix

$$M_{\tilde{\chi}^{\pm}}^2 = \begin{pmatrix} 0 & 0 & M_W & g_2 v_1 \\ 0 & 0 & g_2 v_2 & \lambda v_S \\ M_W & g_2 v_2 & 0 & 0 \\ g_2 v_1 & \lambda v_S & 0 & 0 \end{pmatrix}. \quad (\text{B5})$$

From the diagonalization we get the squared eigenvalues

$$m_{\tilde{\chi}_{1,2}^{\pm}}^2 = \frac{1}{2}[M_W^2 + \lambda^2 v_S^2 + g_2^2 v^2 \mp \sqrt{(M_W^2 + \lambda^2 v_S^2 + g_2^2 v^2)^2 - 4(\lambda v_S M_W - g_2^2 v_1 v_2)^2}]. \quad (\text{B6})$$

If we define

$$\psi^+ = \begin{pmatrix} \lambda_{w^+} \\ \tilde{H}_2^1 \end{pmatrix}, \quad \psi^- = \begin{pmatrix} \lambda_{w^-} \\ \tilde{H}_1^2 \end{pmatrix}, \quad (\text{B7})$$

and define the mass eigenstates as

$$\chi^+ = V\psi^+, \quad \chi^- = U\psi^-, \quad (\text{B8})$$

where U and V are two unitary matrices that perform the diagonalization of this sector. If we define

$$X = \begin{pmatrix} M_W & g_2 v_2 \\ g_2 v_1 & \lambda v_S \end{pmatrix}, \quad (\text{B9})$$

then these unitary matrices are defined in such a way that

$$VX^\dagger XV^{-1} = U^* X X^\dagger U^T = M_{\tilde{\chi}^{\pm}, \text{diag}}, \quad (\text{B10})$$

where $M_{\tilde{\chi}^{\pm}, \text{diag}}$ is given by

$$M_{\tilde{\chi}^{\pm}, \text{diag}} = \begin{pmatrix} m_{\tilde{\chi}_1^{\pm}} & 0 \\ 0 & m_{\tilde{\chi}_2^{\pm}} \end{pmatrix}. \quad (\text{B11})$$

APPENDIX C: RELIC DENSITIES AT THE SECOND MISALIGNMENT

In this Appendix we fill in the gaps in the derivation of the expression of the abundances generated by the mechanism of vacuum misalignment. We start from the Lagrangian

$$S = \int d^4x \sqrt{g} \left(\frac{1}{2} \dot{\chi}^2 - \frac{1}{2} m_\chi^2 \Gamma_\chi \dot{\chi} \right), \quad (\text{C1})$$

where Γ_χ is the decay rate of the axion and we have expanded the potential around its minimum up to quadratic terms. The same action is derived from the quadratic approximation to the general expression

$$S = \int d^4x R^3(t) \left(\frac{1}{2} \sigma_\chi^2 (\partial_\alpha \theta)^2 - \mu^4 (1 - \cos \theta) - V_0 \right), \quad (\text{C2})$$

which, in our case, is constructed from the expression of V' given in Eq. (33), with $\mu \sim v$, the electroweak scale. We also set other contributions to the vacuum potential to vanish ($V_0 = 0$). In a Friedmann-Robertson-Walker space-time metric with a scaling factor $R(t)$, this action gives the equation of motion

$$\frac{d}{dt} [R^3(t)(\dot{\chi} + \Gamma_\chi)] + R^3 m_\chi^2(T) = 0. \quad (\text{C3})$$

We will neglect the decay rate of the axion in this case and set $\Gamma_\chi \approx 0$. At this point, since the potential V' is of nonperturbative origin, we can assume that it vanishes far above the electroweak scale (or temperature T_{EW}). For this reason $m_\chi = m_b = 0$ for $T \gg T_{\text{EW}}$, which is essentially equivalent to assume that the Stückelberg axion is not subject to any mixing far above the weak scale. The general equation of motion derived from Eq. (C3), introducing a temperature dependent mass, can be written as

$$\ddot{\chi} + 3H\dot{\chi} + m_\chi^2(T)\chi = 0, \quad (\text{C4})$$

which clearly allows as a solution a constant value of the misalignment angle $\theta = \theta_i$. The T dependence of the mass term should be generated, for consistency, from a generalization to finite temperature of V' . In practice this is not necessary in our case, being the role of the first misalignment negligible in determining the final mass of the axion. The axion energy density is given by

$$\rho = \frac{1}{2} \dot{\chi}^2 + \frac{1}{2} m_\chi^2 \chi^2, \quad (\text{C5})$$

which after a harmonic averaging gives

$$\langle \rho \rangle = m_\chi^2 \langle \chi^2 \rangle. \quad (\text{C6})$$

Notice that after differentiating Eq. (C5) and using the equation of motion in (C4), followed by the averaging Eq. (C6) one obtains the relation

$$\langle \dot{\rho} \rangle = \langle \rho \rangle \left(-3H + \frac{\dot{m}}{m} \right), \quad (\text{C7})$$

where the time dependence of the mass is through its temperature $T(t)$, while $H(t) = \dot{R}(t)/R(t)$ is the Hubble parameter. By inspection one easily finds that the solution of this equation is of the form

$$\langle \rho \rangle = \frac{m_\chi(T)}{R^3(t)} \quad (\text{C8})$$

showing a dilution of the energy density with an increasing space volume, valid even for a T -dependent mass. At this point, the universe must be (at least) as old as the required period of oscillation in order for the axion field to start oscillating and to appear as dark matter, otherwise θ is misaligned but frozen; this is the content of the condition

$$m_\chi(T_i) = 3H(T_i), \quad (\text{C9})$$

which allows one to identify the initial temperature of the coherent oscillation of the axion field χ , T_i , by equating $m_\chi(T)$ to the Hubble rate, taken as a function of temperature.

To quantify the relic densities at the current temperature T_0 [$T_0 \equiv T(t_0)$, at current time t_0] we define preliminarily the two standard effective couplings

$$\begin{aligned} g_{*,S,T} &= \sum_B g_i \left(\frac{T_i}{T} \right)^3 + \frac{7}{8} \sum_F g_i \left(\frac{T_i}{T} \right)^3, \\ g_{*,T} &= \sum_B g_i \left(\frac{T_i}{T} \right)^4 + \frac{7}{8} \sum_F g_i \left(\frac{T_i}{T} \right)^4, \end{aligned} \quad (\text{C10})$$

functions of the massless relativistic degrees of freedom of the primordial state, with $T \gg T_{\text{EW}}$. The counting of the degrees of freedom is 2 for a Majorana fermion and for a massless gauge boson, 3 for a massive gauge boson, and 1 for a real scalar. In the radiation era, the thermodynamics of all the components of the primordial state is entirely determined by the temperature T , being the system at equilibrium. We exclude for simplicity all sorts of possible sources of entropy due to any inhomogeneity (see, for instance, [55]). Pressure and entropy are then given as a function of the temperature

$$\rho = 3p = \frac{\pi^2}{30} g_{*,T} T^4, \quad s = \frac{2\pi^2}{45} g_{*,S,T} T^3, \quad (\text{C11})$$

while the Friedmann equation allows one to relate the Hubble parameter and the energy density

$$H = \sqrt{\frac{8}{3} \pi G_N \rho}, \quad (\text{C12})$$

with $G_N = 1/M_P^2$ being the Newton constant and M_P the Planck mass. The number density of axions n_χ decreases as

$1/R^3$ with the expansion, as does the entropy density $s \equiv S/R^3$, where S indicates the comoving entropy density—which remains constant in time ($\dot{S} = 0$)—leaving the ratio $Y_a \equiv n_\chi/s$ conserved. We define, as usual, the abundance variable of χ

$$Y_\chi(T_i) = \frac{n_\chi}{s} \Big|_{T_i} \quad (\text{C13})$$

at the temperature of oscillation T_i , and observe that at the beginning of the oscillations the total energy density is the potential one

$$\rho_\chi = n_\chi(T_i) m_\chi(T_i) = 1/2 m_\chi^2(T_i) \chi_i^2. \quad (\text{C14})$$

We then obtain for the initial abundance at $T = T_i$

$$Y_\chi(T_i) = \frac{1}{2} \frac{m_\chi(T_i) \chi_i^2}{s} = \frac{45 m_\chi(T_i) \chi_i^2}{4 \pi^2 g_{*,S,T} T_i^3}, \quad (\text{C15})$$

where we have inserted at the last stage the expression of the entropy of the system at the temperature T_i given by Eq. (C11). At this point, plugging the expression of ρ given in Eq. (C11) into the expression of the Hubble rate as a function of density given in Eq. (C12), the condition for oscillation Eq. (C9) allows one to express the axion mass at $T = T_i$ in terms of the effective massless degrees of freedom evaluated at the same temperature; that is

$$m_\chi(T_i) = \sqrt{\frac{4}{5} \pi^3 g_{*,T_i} \frac{T_i^2}{M_P}}. \quad (\text{C16})$$

This gives for Eq. (C15) the expression

$$Y_\chi(T_i) = \frac{45 \sigma_\chi^2 \theta_i^2}{2 \sqrt{5} \pi g_{*,T_i} T_i M_P}, \quad (\text{C17})$$

where we have expressed χ in terms of the angle of misalignment θ_i at the temperature when oscillations start. We assume that $\theta_i = \langle \theta \rangle$ is the zero mode of the initial misalignment angle after an averaging. As we have already mentioned, T_i should be determined consistently by Eq. (C9). However, the presence of two significant and unknown variables in the expression of m_χ , which are the coupling of the anomalous U(1), g_B , and the Stückelberg mass M , forces us to consider the analysis of the T dependence of χ phenomenologically less relevant. It is more so if the Stückelberg mass is somehow close to the TeV region, in which case the zero temperature axion mass m_χ acquires corrections proportional to the bare coupling [$m_\chi \sim \lambda v(1 + O(g_B))$].

For this reason, assuming that the oscillation temperature T_i is close to the electroweak temperature T_{EW} , Eq. (C16) provides an upper bound for the mass of the axion at which the oscillations occur, assuming that they start around the electroweak phase transition. Stated differently, mass values of χ such that $m(T_i) \ll 3H(T_i)$ correspond to frozen degrees of freedom of the axion at the

electroweak scale. This is clearly an approximation, but it allows one to define the oscillation mass in terms of the Hubble parameter for each given temperature.

We recall that the relic density due to misalignment can be extracted from the relations

$$\Omega_\chi^{\text{mis}} \equiv \frac{\rho_\chi^{\text{mis}}}{\rho_c} = \frac{(n_{\chi 0} m_\chi)}{\rho_c} = \left(\frac{n_{\chi 0}}{s_0} \right) \frac{m_\chi s_0}{\rho_c}, \quad (\text{C18})$$

where we have denoted with $n_{\chi 0}$ the current number density of axions and with ρ_χ^{mis} their current energy density due to vacuum misalignment. This expression can be rewritten as

$$\Omega_\chi^{\text{mis}} = \frac{n_\chi}{s} \bigg|_{T_i} m_\chi \frac{s_0}{\rho_c} \quad (\text{C19})$$

using the conservation of the abundance $Y_{a0} = Y_a(T_i)$. Notice that in Eq. (C19) we have neglected a possible dilution factor $\gamma = s_{\text{osc}}/s_0$ which may be present due to entropy release. We have introduced the variable

$$\rho_c = \frac{3H_0^2}{8\pi G_N}, \quad (\text{C20})$$

which is the critical density and

$$s_0 = \frac{2\pi^2}{45} g_{*S, T_0} T_0^3, \quad (\text{C21})$$

which is the current entropy density. To fix g_{*S, T_0} we recall that at the current temperature T_0 the relativistic species contributing to the entropy density s_0 are the photons and three families of neutrinos with

$$g_{*S, T_0} = 2 + \frac{7}{8} \times 3 \times 2 \left(\frac{T_\nu}{T_0} \right)^3, \quad (\text{C22})$$

where, from entropy considerations, $T_\nu/T_0 = (4/11)^{1/3}$.

To proceed with the computation of the massless degrees of freedom above the electroweak phase transition we recall the structure of the model. We have 13 gauge bosons corresponding to the gauge group $SU(3) \times SU(2) \times U_Y(1) \times U_B(1)$, 2 Higgs doublets, 3 generations of leptons, and 3 families of quarks. Above the energy of the electroweak transition we have only massless fields with the exception of the $U_B(1)$ gauge boson, since this symmetry takes the Stückelberg form above the electroweak scale, giving $g_{*T} = 110.75$. Below the same scale this number is similarly computed with $g_{*T} = 91.25$. Other useful parameters are the critical density and the current entropy

$$\rho_c = 5.2 \times 10^{-6} \text{ GeV/cm}^3, \quad s_0 = 2970 \text{ cm}^{-3}, \quad (\text{C23})$$

with $\theta_i \simeq 1$. It is clear by inserting these numbers into Eq. (C18) that Ω_χ^{mis}

$$\frac{45\sigma_\chi^2 \theta_i^2}{2\sqrt{5}\pi g_{*T_i} T_i M_P} \frac{m_\chi s_0}{\rho_c} \quad (\text{C24})$$

is negligible unless $\sigma_\chi \sim M_{\text{St}}^2/\nu$ is of the same order of $f_a \sim 10^{12}$ GeV, the standard PQ constant. This choice would correspond to $\Omega_\chi \sim 0.1$, but the value of M_{St} should be of $O(10^7)$ GeV.

-
- [1] R. D. Peccei and H. R. Quinn, *Phys. Rev. D* **16**, 1791 (1977).
 [2] R. D. Peccei, *Lect. Notes Phys.* **741**, 3 (2008).
 [3] S. Weinberg, *Phys. Rev. Lett.* **40**, 223 (1978).
 [4] F. Wilczek, *Phys. Rev. Lett.* **40**, 279 (1978).
 [5] M. Dine, W. Fischler, and M. Srednicki, *Phys. Lett.* **104B**, 199 (1981).
 [6] A. R. Zhitnitsky, *Sov. J. Nucl. Phys.* **31**, 260 (1980).
 [7] J. E. Kim, *Phys. Rev. Lett.* **43**, 103 (1979).
 [8] M. A. Shifman, A. I. Vainshtein, and V. I. Zakharov, *Nucl. Phys.* **B166**, 493 (1980).
 [9] A. G. Riess *et al.* (Supernova Search Team), *Astron. J.* **116**, 1009 (1998).
 [10] S. Perlmutter *et al.* (Supernova Cosmology Project), *Astrophys. J.* **517**, 565 (1999).
 [11] Y. Nomura, T. Watari, and T. Yanagida, *Phys. Lett. B* **484**, 103 (2000).
 [12] P. Sikivie, *Lect. Notes Phys.* **741**, 19 (2008).
 [13] S. Chang, C. Hagmann, and P. Sikivie, *arXiv:hep-ph/9812327*.
 [14] E. Arik *et al.* (CAST Collaboration), *J. Cosmol. Astropart. Phys.* **02** (2009) 008.
 [15] S. J. Asztalos *et al.* (ADMX Collaboration), *Phys. Rev. Lett.* **104**, 041301 (2010).
 [16] L. D. Duffy and K. van Bibber, *New J. Phys.* **11**, 105008 (2009).
 [17] G. G. Raffelt, *Lect. Notes Phys.* **741**, 51 (2008).
 [18] L. Visinelli and P. Gondolo, *Phys. Rev. D* **80**, 035024 (2009).
 [19] M. Ahlers, H. Gies, J. Jaeckel, J. Redondo, and A. Ringwald, *Phys. Rev. D* **77**, 095001 (2008).
 [20] M. Ahlers, H. Gies, J. Jaeckel, J. Redondo, and A. Ringwald, *Phys. Rev. D* **76**, 115005 (2007).
 [21] A. De Angelis, O. Mansutti, and M. Roncadelli, *Phys. Lett. B* **659**, 847 (2008).
 [22] A. De Angelis, O. Mansutti, and M. Roncadelli, *Phys. Rev. D* **76**, 121301 (2007).
 [23] A. Mirizzi and D. Montanino, *J. Cosmol. Astropart. Phys.* **12** (2009) 004.
 [24] Z. G. Berezhiani, A. S. Sakharov, and M. Y. Khlopov, *Sov. J. Nucl. Phys.* **55**, 1063 (1992).
 [25] Z. G. Berezhiani, M. Y. Khlopov, and A. S. Sakharov, Report No. DFTUZ-91-29.

- [26] C. Corianò, N. Irges, and S. Morelli, *J. High Energy Phys.* **07** (2007) 008.
- [27] C. Corianò, N. Irges, and S. Morelli, *Nucl. Phys.* **B789**, 133 (2008).
- [28] J. De Rydt, J. Rosseel, T. T. Schmidt, A. Van Proeyen, and M. Zagermann, *Classical Quantum Gravity* **24**, 5201 (2007).
- [29] J.-P. Derendinger, P. M. Petropoulos, and N. Prezas, *Nucl. Phys.* **B785**, 115 (2007).
- [30] C. Corianò, M. Guzzi, G. Lazarides, and A. Mariano, *Phys. Rev. D* **82**, 065013 (2010).
- [31] B. de Carlos, J. A. Casas, F. Quevedo, and E. Roulet, *Phys. Lett. B* **318**, 447 (1993).
- [32] T. Banks, M. Dine, and M. Graesser, *Phys. Rev. D* **68**, 075011 (2003).
- [33] C. Corianò, N. Irges, and E. Kiritsis, *Nucl. Phys.* **B746**, 77 (2006).
- [34] C. Corianò, M. Guzzi, A. Mariano, and S. Morelli, *Phys. Rev. D* **80**, 035006 (2009).
- [35] C. Corianò, M. Guzzi, N. Irges, and A. Mariano, *Phys. Lett. B* **671**, 87 (2009).
- [36] M. Cvetič, D. A. Demir, J. R. Espinosa, L. L. Everett, and P. Langacker, *Phys. Rev. D* **56**, 2861 (1997).
- [37] P. Anastasopoulos, F. Fucito, A. Lionetto, G. Pradisi, A. Racioppi, and Y. S. Stanev, *Phys. Rev. D* **78**, 085014 (2008).
- [38] F. Fucito, A. Lionetto, A. Mammarella, and A. Racioppi, *Eur. Phys. J. C* **69**, 455 (2010).
- [39] A. Lionetto and A. Racioppi, *Nucl. Phys.* **B831**, 329 (2010).
- [40] C. Corianò, M. Guzzi, and S. Morelli, *Eur. Phys. J. C* **55**, 629 (2008).
- [41] C. Corianò and M. Guzzi, *Nucl. Phys.* **B826**, 87 (2010).
- [42] B. Kors and P. Nath, *J. High Energy Phys.* **12** (2004) 005.
- [43] R. Armillis, C. Corianò, M. Guzzi, and S. Morelli, *Nucl. Phys.* **B814**, 156 (2009).
- [44] C. Corianò, A. E. Faraggi, and M. Guzzi, *Phys. Rev. D* **78**, 015012 (2008).
- [45] S. Chatrchyan *et al.* (CMS Collaboration), *J. High Energy Phys.* **05** (2011) 093.
- [46] G. Aad *et al.* (ATLAS Collaboration), *Phys. Rev. Lett.* **107**, 272002 (2011).
- [47] N. D. Christensen and C. Duhr, *Comput. Phys. Commun.* **180**, 1614 (2009).
- [48] A. Pukhov, [arXiv:hep-ph/0412191](https://arxiv.org/abs/hep-ph/0412191).
- [49] G. Belanger, F. Boudjema, P. Brun, A. Pukhov, S. Rosier-Lees, P. Salati, and A. Semenov, *Comput. Phys. Commun.* **182**, 842 (2011).
- [50] S. Chatrchyan *et al.* (CMS Collaboration), [arXiv:1202.1488](https://arxiv.org/abs/1202.1488).
- [51] G. Aad *et al.* (ATLAS Collaboration), *Phys. Lett. B* **710**, 49 (2012).
- [52] N. Jarosik *et al.*, *Astrophys. J. Suppl. Ser.* **192**, 14 (2011).
- [53] E. F. Ribas (CAST Collaboration), [arXiv:0912.4222](https://arxiv.org/abs/0912.4222).
- [54] D. Feldman, Z. Liu, P. Nath, and G. Peim, *Phys. Rev. D* **81**, 095017 (2010).
- [55] G. Lazarides, R. K. Schaefer, D. Seckel, and Q. Shafi, *Nucl. Phys.* **B346**, 193 (1990).